



Article

Molecular and Cytogenetic Analysis of rDNA Evolution in *Crepis Sensu Lato*

Magdalena Senderowicz¹, Teresa Nowak¹, Hanna Weiss-Schneeweiss² , Laszlo Papp³ and Bozena Kolano^{1,*}

¹ Institute of Biology, Biotechnology and Environmental Protection, Faculty of Natural Sciences, University of Silesia in Katowice, 40-007 Katowice, Poland; senderowicz.magdalena@gmail.com (M.S.); teresa.nowak@us.edu.pl (T.N.)

² Department of Botany and Biodiversity Research, University of Vienna, Rennweg 14, A-1030 Vienna, Austria; hanna.schneeweiss@univie.ac.at

³ Eötvös Loránd University Botanical Garden, Illés u. 25, 1083 Budapest, Hungary; papplaca@gmail.com

* Correspondence: bozena.kolano@us.edu.pl; Tel.: +483-2200-9468

Abstract: Although *Crepis* was the first model plant group in which chromosomal changes were considered to play an important role in speciation, their chromosome structure and evolution have been barely investigated using molecular cytogenetic methods. The aim of the study was to provide a better understanding of the patterns and directions of *Crepis* chromosome evolution, using comparative analyses of rDNA loci number and localisation. The chromosome base number and chromosomal organisation of 5S and 35S rDNA loci were analysed in the phylogenetic background for 39 species of *Crepis*, which represent the evolutionary lineages of *Crepis sensu stricto* and *Lagoseris*, including *Lapsana communis*. The phylogenetic relationships among all the species were inferred from nrITS and newly obtained 5S rDNA NTS sequences. Despite high variations in rDNA loci chromosomal organisation, most species had a chromosome with both rDNA loci within the same (usually short) chromosomal arm. The comparative analyses revealed several independent rDNA loci number gains and loci repositioning that accompanied diversification and speciation in *Crepis*. Some of the changes in rDNA loci patterns were reconstructed for the same evolutionary lineages as descending dysploidy.

Keywords: rDNA loci; *Crepis*; 5S rDNA NTS; nrITS; chromosomes; FISH; phylogeny



Citation: Senderowicz, M.; Nowak, T.; Weiss-Schneeweiss, H.; Papp, L.; Kolano, B. Molecular and Cytogenetic Analysis of rDNA Evolution in *Crepis Sensu Lato*. *Int. J. Mol. Sci.* **2022**, *23*, 3643. <https://doi.org/10.3390/ijms23073643>

Academic Editor: Frank M. You

Received: 21 February 2022

Accepted: 24 March 2022

Published: 26 March 2022

Publisher's Note: MDPI stays neutral with regard to jurisdictional claims in published maps and institutional affiliations.



Copyright: © 2022 by the authors. Licensee MDPI, Basel, Switzerland. This article is an open access article distributed under the terms and conditions of the Creative Commons Attribution (CC BY) license (<https://creativecommons.org/licenses/by/4.0/>).

1. Introduction

Changes in the karyotype structure, which often accompany diversification and speciation events, are a focal point of plant evolutionary studies [1–3]. Chromosomal rearrangements are not only associated with changes in the size and structure of chromosomes but also with changes in the chromosome base numbers via ascending or descending dysploidy [1,2,4]. The dysploid chromosomal changes have been inferred for many species of Asteraceae [5] and other plant families (e.g., Fabaceae [6]). The patterns and mechanisms of karyotype evolution have been most extensively studied in two plant families that include model species, Poaceae (e.g., *Brachypodium dystachion* and *Oryza sativa*) [3,7–9] and Brassicaceae (*Arabidopsis thaliana* [10–12]). Analyses of the localisation of the BACs (bacterial artificial chromosomes) using FISH (fluorescent in situ hybridisation) has demonstrated that different types of chromosomal rearrangements, which are often group-specific, accompanied the evolution of their karyotypes. Inversions and translocations were detected as the most frequent types of chromosomal rearrangements in the Brassicaceae family [11], whereas, in *Brachypodium* (Poaceae), descending dysploidy has been inferred to have occurred primarily via nested chromosomal fusions [7,8]. The use of FISH with oligo probes that are specific for selected regions of individual chromosomes enabled the occurrence of the reciprocal chromosomal translocations that accompanied the evolution and speciation of two *Solanum* species to be demonstrated [13]. These approaches, however, can only be used in taxa, for which whole-genome assemblies for at least one member of the analysed

group is available [7,14]. In non-model species, comparative analyses of chromosome structure and karyotype evolution usually rely on FISH with various repetitive sequences as the probes [15,16]. Comparative mapping of chromosomal markers might enable at least some chromosomal rearrangements to be identified and thus enable a better understanding of the patterns of their chromosomal evolution [17,18]. 5S and 35S rDNAs are most often used as chromosomal markers, as they are highly repetitive, arranged in tandem arrays and highly conserved in the DNA sequence of the coding regions [19–23]. The non-transcribed spacer (NTS) of 5S rDNA and the internal transcribed spacer of 35SrDNA (nrITS 1 and 2) evolve much faster than their coding regions and are thus often used as molecular markers in phylogenetic analyses [24]. In most higher plants, the number and localisation of the 35S and 5S rDNA loci are unlinked [25].

Crepis species are mostly diploids with chromosome base numbers of $x = 3, 4, 5, 6$ and 11. Three evolutionary lineages were identified in *Crepis sensu lato* (s.l.): (i) *Crepis* species with a chromosome base number $x = 7$, now the genus *Askellia*; (ii) *Lagoseris*, which encompasses several *Crepis* species (e.g., *C. palaestina* and *C. praemorsa*) and two other lineages, which are now classified as the genera *Lapsana* and *Rhagadiolus*, and (iii) *Crepis sensu stricto* (*Crepis s.s.* [26,27]). The chromosomes of *Crepis* species are relatively large and well-differentiated within the karyotype [27,28]. Analyses of the chromosome numbers and karyotype structure in phylogenetic framework inferred $x = 6$ as an ancestral state for *Crepis s.l.* Several subsequent and independent descending dysploidy events led to the evolution of derived chromosome base numbers ($x = 5, 4, 3$) during the diversification of the genus [27]. Most of the currently accepted clades of closely related *Crepis* species include taxa that differ in chromosome numbers and karyotype morphology [26,27].

Molecular cytogenetic analyses of *Crepis* karyotypes are scarce and usually encompass fluorochrome banding and the localisation of a few repetitive DNA sequences using FISH. The chromosomal organisation of two satellite DNA sequences (pCcD32 and pCcE9) has only been analysed in the *C. capillaris* genome ($2n = 6$) and revealed chromosome-specific hybridisation patterns of these two repeats [29]. The chromosomal organisation of the rRNA gene loci was studied in *C. capillaris* ($2n = 6$) and three closely related species from the section *Neglectoides*: *C. neglecta* ($2n = 8$), *C. cretica* ($2n = 8$) and *C. hellenica* ($2n = 6$ [30]). In *C. capillaris*, one locus of each of the 35S and 5S rDNAs were observed [31,32]. Both rDNA loci were located in the short arm of the subtelocentric chromosome, with the 35S rDNA locus in a more distal position. In the other three species, to the subtelocentric chromosome that carried both the 35S and 5S rDNA loci and an additional second locus of 35S rDNA in the pericentromeric region of another chromosome were observed [30].

The aims of this study were to analyse the chromosomal organisation and evolution of the rDNA loci in 39 *Crepis* species belonging to the *Crepis s.s.* and *Lagoseris* evolutionary lineages; the latter also includes *Lapsana communis*. The specific objectives were to (1) establish the number and localisation of the 5S and 35S rDNA loci in all of the analysed species, most for the first time, (2) to reconstruct the ancestral states of the 5S and 35S rDNA loci numbers for the genus and (3) to infer the patterns and directionality of the rDNA loci evolution within the phylogenetic framework that is inferred from the analyses of the nrITS [27]. Double fluorochrome banding with CMA₃ and DAPI was used to identify the relationships between the localisation of rDNA loci and the positive CMA₃ bands. The newly generated 5S rDNA sequence data gave insight into the intra- and interspecific polymorphism of the 5S rDNA sequences.

2. Results

2.1. Phylogenetic Analyses of the 5S rDNA NTS and nrITS

Phylogenetic analyses of the 5S rDNA NTS were conducted separately for the *Lagoseris* and *Crepis s.s.* lineages due to the high levels of sequence divergence. The length of the analysed region ranged from 252 to 353 bp among all of the analysed *Crepis* species and from 673 to 677 bp in *L. communis*. The alignment of the *Lagoseris* sequences was 738 bp long with 192 parsimony informative sites, whereas the alignment of the *Crepis s.s.* se-

quences was 446 bp long with 364 parsimony informative sites. The inferred phylogenetic relationships revealed two main groups in *Lagoseris* (Figures 1 and S1). The first group consisted solely of *L. communis* (BS99), whereas the second comprised the remaining five species of this lineage. These species formed three groups that were identified as: (i) a clade consisting of *C. sancta* and *C. magellensis* (BS99), (ii) a clade consisting of *C. praemorsa* (BS100) and (iii) a clade consisting of *C. palaestina* and *C. pulchra* (Figure 1).

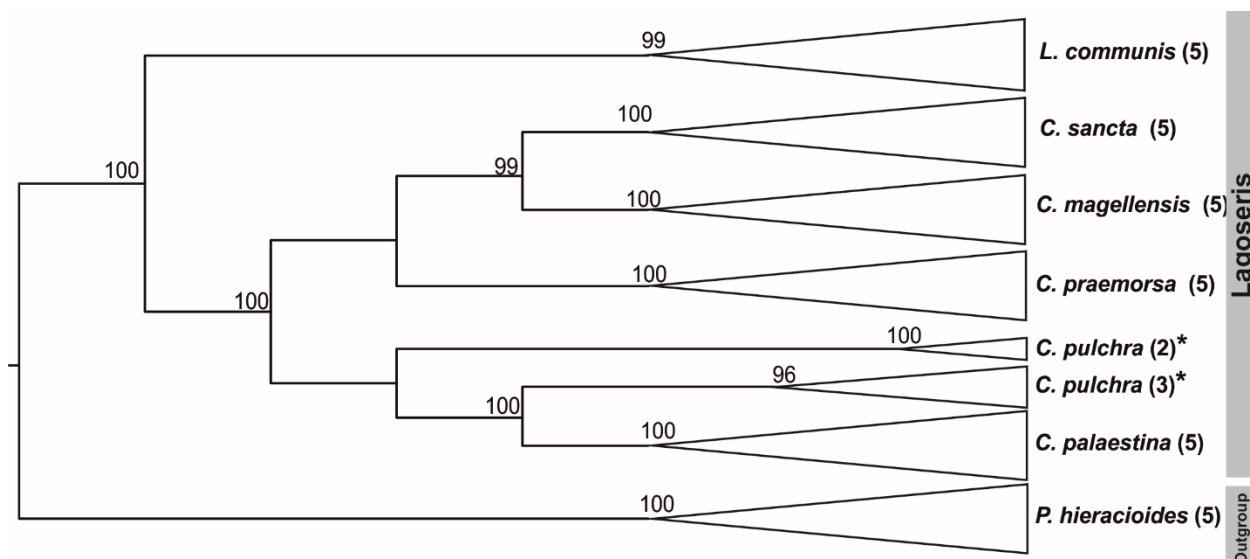


Figure 1. Phylogenetic analysis of cloned sequences of the 5S rDNA non-transcribed spacer representing species of *Lagoseris* lineage. Numbers in parentheses indicate the number of analysed clones. The tree was rooted with *Picris hieracioides*. Bootstrap scores are shown above branches. The stars indicate species with two variants of 5S rDNA NTS.

All of the analysed species of the *Crepis* s.s. lineage were assigned to 12 clades (Figures 2 and S2). Most of the clades were well-supported, whereas most of the nodes in the backbone of the tree were poorly supported (Figure 2). The clades that were recovered from the 5S rDNA NTS analyses are labelled with capital letters (clades A–K). The first three well-supported clades (clades A–C, all BS100) comprised species with $x = 6$. Clade D (BS100) primarily consisted of perennial species with $x = 4$ (Figures 2 and S2). The remaining clades (E–K) consisted of species with chromosome base numbers of $x = 5$, 4 or 3. Usually, two base chromosome numbers were present in each clade (Figure 2).

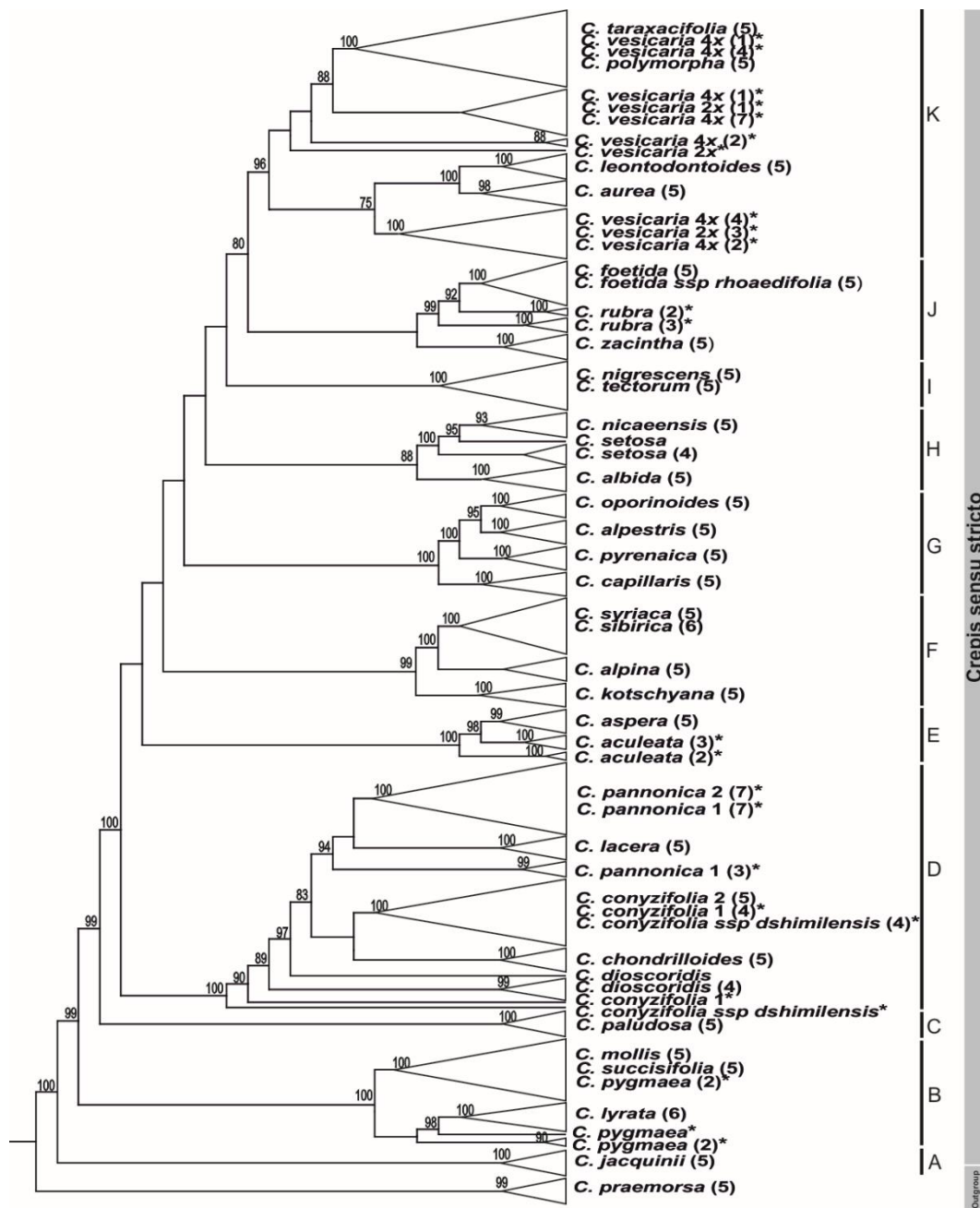


Figure 2. Phylogenetic analysis of the cloned sequences of 5S rDNA non-transcribed spacer representing species of *Crepis* s.s. lineage. Numbers in parentheses indicate the number of clones analysed. The tree was rooted with *C. praemorsa*. Bootstrap scores are shown above branches. Stars indicate species with two variants of 5S rDNA NTS. A–K letters indicates clades. In the ML analysis of the nrITS region, two main well-supported evolutionary lineages were recovered: *Lagoseris* (BS94) and *Crepis* s.s. (BS85; Figure 3). In *Crepis* s.s., four main clades (1–4) that had high bootstrap support (BS72–BS100) were found. The newly sequenced *C. chondrilloides* was recovered in clade 3 (Figure S3).

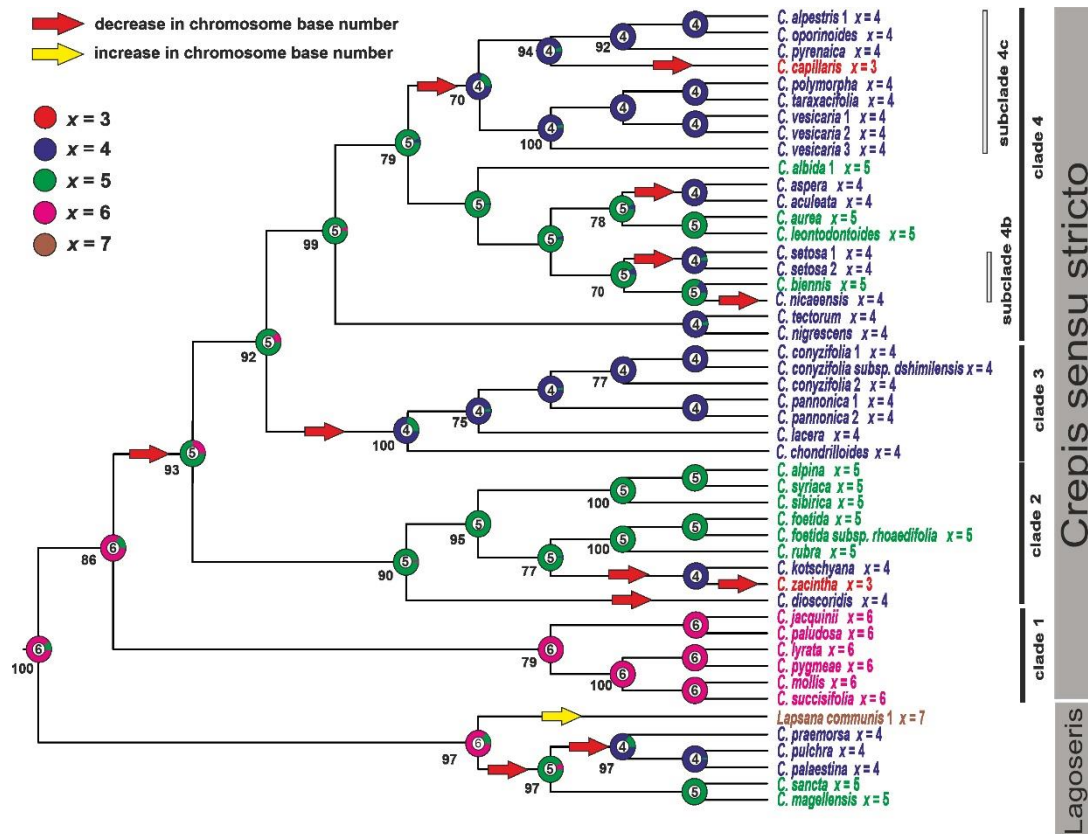


Figure 3. Ancestral character state reconstruction of the chromosome base numbers in *Crepis* s.l. The chromosome base numbers have been mapped on the ML tree resulting from analyses of the nrITS sequences using the maximum likelihood method as implemented in ChromEvol 2.0. The tree was rooted with *Picris hieracioides*, *Lactuca serriola* and *Sonchus oleraceus*. Bootstrap scores are shown below the branches.

2.2. Chromosome Number Evolution

Although the majority of the analysed *Crepis* species had base chromosome numbers of $x = 5$ (ten species) or $x = 4$ (21 species), some species were also found with $x = 6$ and $x = 3$. The $x = 7$ was only observed in *L. communis*. Most of the species were diploid, except for *C. vesicaria*, which had both diploid and tetraploid individuals. The ML analysis (ChromEvol 2.0), which was based on the nrITS datasets, enabled the ancestral chromosome base number for the common ancestor of *Lagoseris* and *Crepis* s.s. to be inferred as $x = 6$ ($pp = 0.86$). The analysis suggested 12 events of decreases (expectation above 0.5) in the chromosome base number, two in the *Lagoseris* lineage and ten in *Crepis* s.s.. Only one increase in the chromosome base number was inferred for *L. communis* in the *Lagoseris* lineage (Figure 3 and Table 1).

Table 1. The number and localisation of the 35S and 5S rDNA loci and CMA₃⁺ bands in *Crepis*.

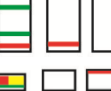
Species	Chromosome Number	Number and Localisation of 35S  and 5S  rDNA Loci and CMA ₃ ⁺  Bands			
		5S rDNA	35S rDNA	CMA ₃ ⁺	
<i>Crepis</i> s.s.					
<i>Crepis aculeata</i>	2n = 2x = 8	1	2		1 (35S rDNA) *
<i>C. albida</i>	2n = 2x = 10	1	1		1 (35S rDNA)
<i>C. alpestris</i>	2n = 2x = 8	1	1		1 (35S rDNA)
<i>C. alpina</i>	2n = 2x = 10	1	1		1 (35S rDNA)
<i>C. aspera</i>	2n = 2x = 8	2	1		-
<i>C. aurea</i>	2n = 2x = 10	1	1		2 (1 with 35S & 1 with 5S rDNA)
<i>C. capillaris</i>	2n = 2x = 6	1	1		1 (35S rDNA)
<i>C. conyzifolia</i> (1)	2n = 2x = 8	3	4		1 (35S rDNA)
<i>C. conyzifolia</i> (2)	2n = 2x = 8	3	4		1 (35S rDNA)
<i>C. conyzifolia</i> subsp. <i>dshimilensis</i> (3)	2n = 2x = 8	2	4		1 (35S rDNA)
<i>C. chondrilloides</i>	2n = 2x = 8	1	3		-
<i>C. dioscoridis</i>	2n = 2x = 8	2	2		3 (2 with 35S & 1 with 5S rDNA)
<i>C. foetida</i> (1)	2n = 2x = 10	1	1		1 (35S rDNA)
<i>C. foetida</i> subsp. <i>rhoaedifolia</i> (2)	2n = 2x = 10	3	1		1 (35S rDNA)

Table 1. Cont.

Species	Chromosome Number	Number and Localisation of 35S  and 5S  rDNA Loci and CMA ₃ ⁺  Bands		
		5S rDNA	35S rDNA	CMA ₃ ⁺
<i>C. jacquinii</i>	2n = 2x = 12	1	1	 -
<i>C. kotschyana</i>	2n = 2x = 8	1	1	 1 (35S rDNA)
<i>C. lacera</i>	2n = 2x = 8	2	1	 2 (1 with 35S & 1 with 5S rDNA)
<i>C. leontodontoides</i>	2n = 2x = 10	1	1	 1 (35S rDNA)
<i>C. lyrata</i>	2n = 2x = 12	1	1	 1 (35S rDNA)
<i>C. mollis</i>	2n = 2x = 12	2	1	 1 (35S rDNA)
<i>C. nicaeensis</i>	2n = 2x = 8	1	2	 -
<i>C. nigrescens</i>	2n = 2x = 8	1	1	 -
<i>C. oporinoides</i>	2n = 2x = 8	1	2	 1 (35S rDNA)
<i>C. paludosa</i>	2n = 2x = 12	1	1	 1 (35S rDNA)
<i>C. pannonica</i> (1)	2n = 2x = 8	2	3	 2 (35S rDNA)
<i>C. pannonica</i> (2)	2n = 2x = 8	3	4	 -
<i>C. polymorpha</i>	2n = 2x = 8	2	1	 -
<i>C. pygmaea</i>	2n = 2x = 12	3	1	 1 (35S rDNA)

Table 1. Cont.

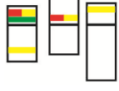
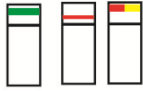
Species	Chromosome Number	Number and Localisation of 35S  and 5S  rDNA Loci and CMA ₃ ⁺  Bands		
		5S rDNA	35S rDNA	CMA ₃ ⁺
<i>C. pyrenaica</i>	2n = 2x = 8	1	1	 1 (35S rDNA)
<i>C. rubra</i>	2n = 2x = 10	1	2	 4 (2 with 35S rDNA)
<i>C. setosa</i> 1	2n = 2x = 8	1	1 + (1)	 1 (35S rDNA)
<i>C. setosa</i> 2	2n = 2x = 8	1	1 or 2	 1 (35S rDNA)
<i>C. sibirica</i>	2n = 2x = 10	1	1	 -
<i>C. succisifolia</i>	2n = 2x = 12	2	1	 1 (35S rDNA)
<i>C. syriaca</i>	2n = 2x = 10	1	1	 1 (35S rDNA)
<i>C. taraxacifolia</i>	2n = 2x = 8	2	1	 1 (35S rDNA)
<i>C. tectorum</i>	2n = 2x = 8	1	1	 1 (35S rDNA)
<i>C. vesicaria</i> (3)	2n = 2x = 8	2	1	 1 (35S rDNA)
<i>C. vesicaria</i> (1)	2n = 4x = 16	2	1	 2 (35S rDNA)
<i>C. vesicaria</i> (2)	2n = 4x = 16	2	1	 2 (35S rDNA)
<i>C. zacintha</i>	2n = 2x = 6	1	1	 1 (35S rDNA)

Table 1. Cont.

Species	Chromosome Number	Number and Localisation of 35S  and 5S  rDNA Loci and CMA ₃ ⁺  Bands			
		5S rDNA	35S rDNA	CMA ₃ ⁺	
Lagoseris					
<i>C. magellensis</i>	2n = 2x = 10	1	2		1 (35S rDNA)
<i>C. palaestina</i>	2n = 2x = 8	2	3		2 (35S rDNA)
<i>C. praemorsa</i>	2n = 2x = 8	2	1		-
<i>C. pulchra</i>	2n = 2x = 8	2	2		2 (35S rDNA)
<i>C. sancta</i>	2n = 2x = 10	1	2		2 (35S rDNA)
<i>Lapsana communis</i>	2n = 2x = 14	3	1		1 (35S rDNA)

* The co-localisation of the CMA₃⁺ bands with the rDNA loci are given in parentheses. A parenthesis under the chromosome in the idiograms indicates a polymorphism in the rDNA loci chromosomal organisation.

2.3. Chromosomal Organisation of the rDNA Loci

The number and localisation of the rDNA loci was determined using FISH with 25S and 5S rDNA probes. The rDNA loci number and localisation are reported for 38 *Crepis* species and for *L. communis* for the first time (Table 1). Seventeen analysed diploid *Crepis* species had one locus of each 35S and 5S rDNA (Figures 4J–L, N–U and 5D, E, I, J, L, M, S–V). Nine species had two loci of 35S rDNA (Figures 4B, C, E, P, U and 5B, F, U, K), and only three species had three or four loci of this sequence (Figures 4D, X, Y and 5A–C). Fourteen diploid species had two loci of 5S rDNA (Figures 4D–H, M, W, X and 5B, L, N, Q, R). Three loci of 5S rDNA were observed in both accessions of *C. foetida* and in some of the accessions of *C. conyzifolia* and *C. pannonica* (Figures 4Q, R, Y and 5A, C). *L. communis* (2n = 2x = 14) had three loci of 5S rDNA and one locus of 35S rDNA (Figure 4A; Table 1). The chromosomal organisation of the rDNA loci varied among the analysed species with more than 20 different patterns of the chromosomal distribution of the rDNA loci (Figures 4 and 5 and Table 1). In the *Lagoseris* evolutionary lineage, there was high interspecific polymorphisms in the rDNA loci number and localisation. The number of both the 5S and 35S rDNA loci varied from one to three among these species, with each species having a unique chromosomal pattern of the rDNA loci distribution (Table 1 and Figure 4A–F).

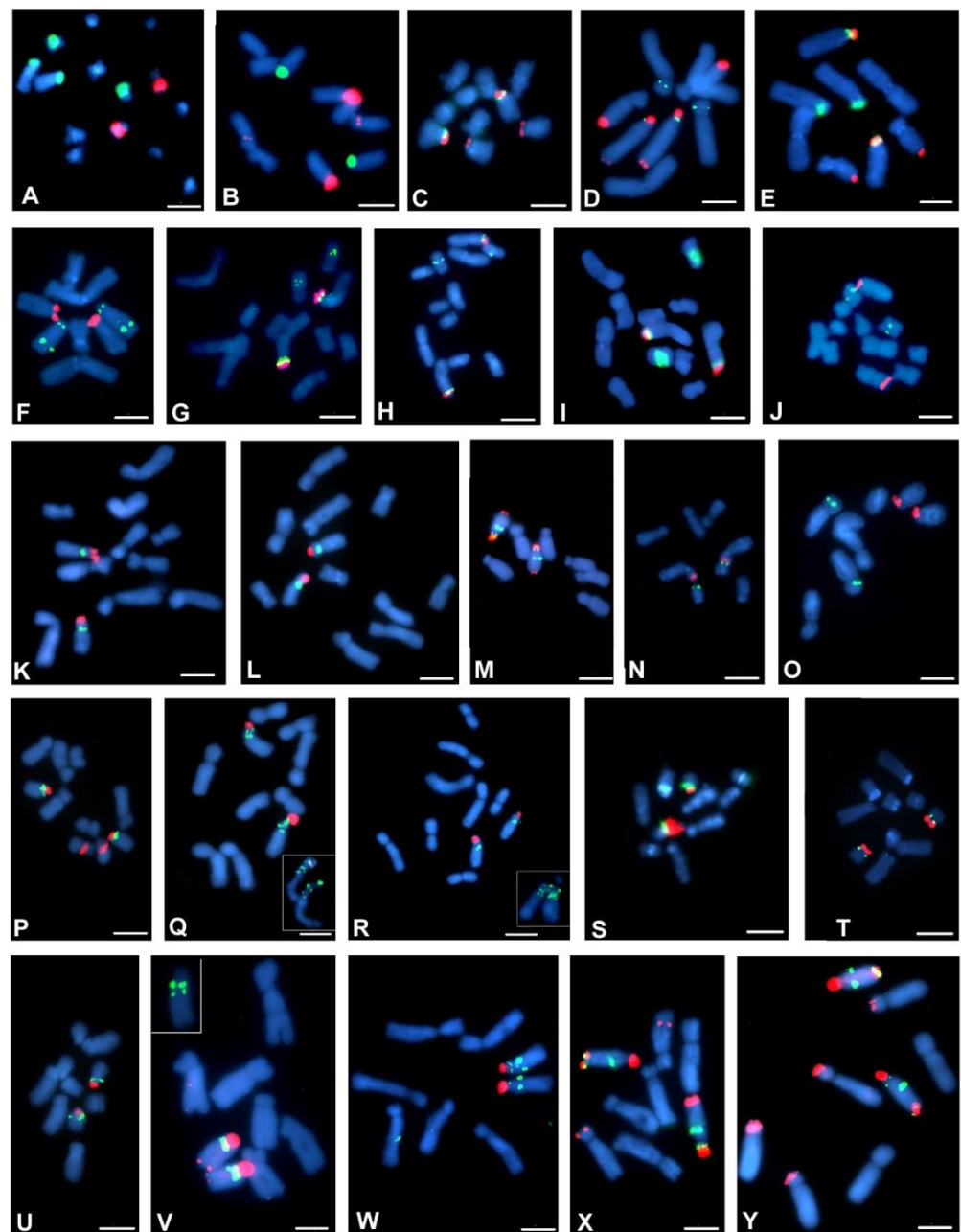


Figure 4. Localisation of 35S and 5S rDNA loci in metaphase chromosomes of *Crepis* species. Fluorescent in situ hybridisation was performed with the 5S rDNA probe (green fluorescence) and 25S rDNA probe (red fluorescence). (A) *Lapsana communis*, (B) *C. magellensis*, (C) *C. sancta*, (D) *C. palaestina*, (E) *C. pulchra*, (F) *C. praemorsa*, (G) *C. succisifolia*, (H) *C. mollis*, (I) *C. pygmaea*, (J) *C. lyrata*, (K) *C. paludosa*, (L) *C. jacquinii*, (M) *C. dioscoridis*, (N) *C. zacintha*, (O) *C. kotschyana*, (P) *C. rubra*, (Q) *C. foetida* subsp. *rhoaedifolia*, (R) *C. foetida*, (S) *C. sibirica*, (T) *C. syriaca*, (U) *C. alpina*, (V) *C. chondrilloides*, (W) *C. lacera*, (X) *C. pannonica* 1 and (Y) *C. pannonica* 2. Scale bar = 5 μ m.

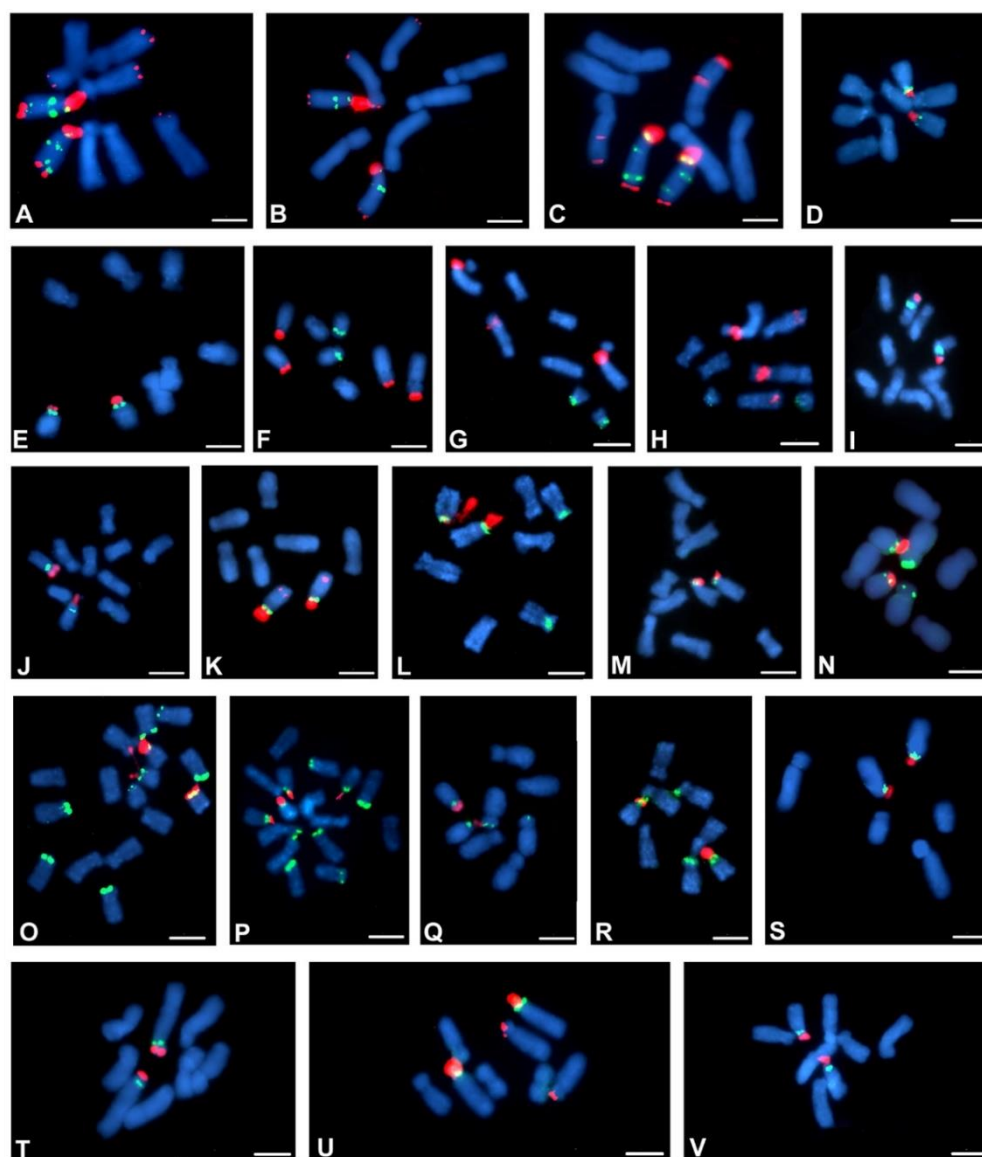


Figure 5. Localisation of 35S and 5S rDNA loci in metaphase chromosomes of *Crepis* species. Fluorescent in situ hybridisation was performed with 5S rDNA (green fluorescence) and 25S rDNA probes (red fluorescence). (A) *C. conyzifolia* 2, (B) *C. conyzifolia* subsp. *dshimilensis*, (C) *C. conyzifolia* 1, (D) *C. nigrescens*, (E) *C. tectorum*, (F) *C. nicaensis*, (G) *C. setosa* 1, (H) *C. setosa* 2, (I) *C. leontodontoides*, (J) *C. aurea*, (K) *C. aculeata*, (L) *C. aspera*, (M) *C. albida*, (N) *C. vesicaria* 3, (O) *C. vesicaria* 2, (P) *C. vesicaria* 1, (Q) *C. taraxacifolia*, (R) *C. polymorpha*, (S) *C. capillaris*, (T) *C. pyrenaica*, (U) *C. oporinoides* and (V) *C. alpestris*. Scale bar = 5 μ m.

In 12 species of the *Crepis* s.s. lineage, karyotypes with one chromosome bearing both rDNA loci within one, usually short, arm and with the locus of 35S rDNA in the more distal position, were observed (Table 1). Such a pattern was also observed in two species of clade 1 (*C. paludosa* and *C. jacquinii*; Figure 4K,L), three species in clade 2 (*C. sibirica*, *C. syriaca* and *C. alpina*; Figure 4S–U) and in eight species from clade 4 (Figure 5D,E,I,J,M,S,V,T). A similar pattern of both the rDNA loci in one chromosomal arm but with 5S rDNA in a more distal position (Figure 4N) was observed in *C. zacintha* karyotype (clade 2). In the karyotype of 16 species of *Crepis* s.s., in addition to the common pattern with both rDNA loci within one chromosome arm with the locus of 35S rDNA in a more distal position, additional locus/loci of 35S and/or 5S rDNA were observed (Figures 4G–J,M,P–S,V–Y and 5A–C,K,L,N,Q,R,U and Table 1). Among them, the species from clade 3 had the relatively highest interspecific polymorphisms in the rDNA loci number and localisation.

Each species had a different pattern of rDNA loci distribution. Although quite variable loci patterns were observed in the species in clade 3, most of them had one chromosome that carried two loci of 35S rDNA and two or three loci of 5S rDNA (Figures 4V,X,Y and 5A–C). In the karyotypes of *C. lyrata* (clade 1; Figure 4J) and three species from subclade 4b (*C. kotschyana*, *C. nicaeensis* and *C. setosa*; Figures 4O and 5F–H), the 5S and 35S rDNA loci were observed in separate chromosomes. *C. vesicaria*, a species with both diploid and tetraploid accessions, had one chromosome bearing both the 35S and 5S rDNA in its short arm and the second locus of 5S rDNA in the short arm of another chromosome in the diploids (Figure 5N). The tetraploid accessions of *C. vesicaria* had the same patterns of loci distribution but with double the number of loci and chromosomes (Figure 5O,P).

Three diploid *Crepis* species had intraspecific polymorphisms of the number and/or localisation of the rDNA sites. A polymorphism of 35S rDNA loci number was observed among the analysed *C. setosa* accessions. Two, three or four hybridisation signals of 35S rDNA were observed (Figure 6A–C and Table 1). Among the analysed *C. conyzifolia* and *C. pannonica* accessions, there were polymorphisms of the chromosomal patterns of both the 35S and 5S rDNA loci (Figure 6D–F and Table 1) that had additional loci of both rDNA types.

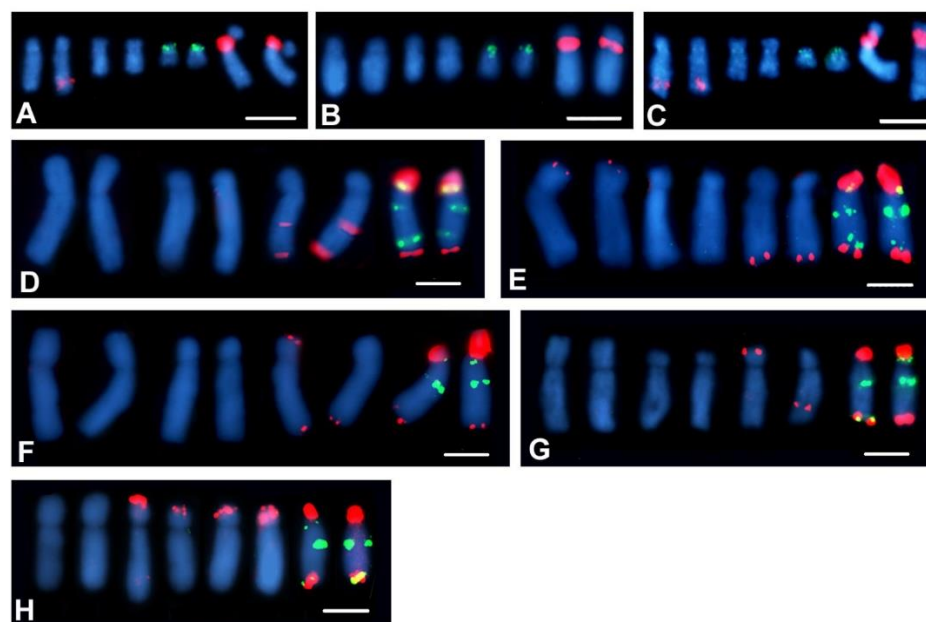


Figure 6. Karyotypes of *Crepis* species showing intraspecific polymorphisms of the rDNA loci number and localisation: (A) *C. setosa* 1, (B) *C. setosa* 2, (C) *C. setosa* 2, (D) *C. conyzifolia* 1, (E) *C. conyzifolia* 2, (F) *C. conyzifolia* subsp. *Dshimilensis*, (G) *C. pannonica* 1 and (H) *C. pannonica* 2. Scale bar = 5 μ m.

2.4. Fluorochrome Banding

Fluorescent staining with CMA₃ was used to detect the GC-rich chromosomal regions [33]. CMA₃ banding was performed for 38 accessions representing 32 *Crepis* species and for *L. communis*. For the 28 *Crepis* species and *L. communis*, only the CMA₃⁺ bands that co-localised with the major locus/loci of 35S rDNA were observed (Table 1 and Figure S4). In *C. aurea*, *C. dioscoridis* and *C. lacera* CMA₃⁺, the bands colocalising with both the 35S rDNA and 5S rDNA loci were detected. In the *C. rubra* karyotype, four pairs of the CMA₃⁺ bands were observed. Two of these were colocalised with the 35S rDNA loci, and two others did not colocalise with either the 35S or with the 5S rDNA loci.

2.5. Patterns of Ribosomal DNA Loci Evolution

The number of rDNA loci was mapped on the ML phylogenetic tree of the nrITS using the maximum likelihood reconstruction methods as implemented in Mesquite (Figure 7). One locus of 5S rDNA was reconstructed as an ancestral state for the Lagoseris and Crepis s.s. lineages (Figure 7A). In the Lagoseris clade, only two species (*C. sancta* and *C. magellensis*) had an ancestral number of loci. The remaining species had two or three loci of 5S rDNA. In the Crepis s.s. lineage, more than half of the analysed species had an ancestral number of 5S rDNA loci. Thirteen events of 5S rDNA loci gains were reconstructed for this evolutionary lineage. Gains of the 5S rDNA loci were inferred for a common ancestor of clade 3 and a common ancestor of the species related to *C. vesicaria* (clade 4). Other gains of 5S rDNA were reconstructed at the tips of the tree (Figure 7A).

Analyses of the 35S rDNA loci numbers resulted in the reconstruction of one locus of 35S rDNA as an ancestral state for a common ancestor of Lagoseris and Crepis s.s. (Figure 7B). Most species of the Lagoseris lineage had a higher number of 35S rDNA loci (two or three loci), and only two species, *C. praemorsa* and *L. communis*, had only one locus (Figure 7B). Conversely, most species of the Crepis s.s. lineage had an ancestral number of 35S rDNA loci, except for clade, 3 in which the majority of species had three or four loci. All of the species in clade 1 and most of the species in clade 2 and clade 4 had an ancestral loci number (Figure 7B). Nine events of 35S rDNA loci gains that had accompanied the speciation or evolution of two closely related species were reconstructed in Crepis s.s. (Figure 7B).

In the karyotypes of the majority of the analysed species, one chromosome consistently carried one of each 35S and 5S rDNA loci in the same, often short, chromosomal arm with 35S rDNA located distally. The presence/absence of this chromosome was mapped on the ML phylogenetic tree of the nrITS using the maximum likelihood reconstruction. The ancestral state that was reconstructed for the Lagoseris lineages was ambiguous (Figure 7C). The analysis resulted in the reconstruction of this arrangement as an ancestral state for Crepis s.s. (Figure 7C). Only three events of rDNA loci repositioning were reconstructed for Crepis s.s. During the evolution of a common ancestor of subclade 4b and the speciation of *C. lyrata* and *C. kotschyana*, the repositioning of the rDNA loci resulted in karyograms with the 5S and 35S rDNA loci in different chromosomes. However, the result of the rDNA loci repositioning during the speciation of *C. zacintha* was a karyotype with both rDNA locus types in one chromosomal arm but in the reverse order of the 5S and 35S rDNA loci (Figure 4N and Table 1).

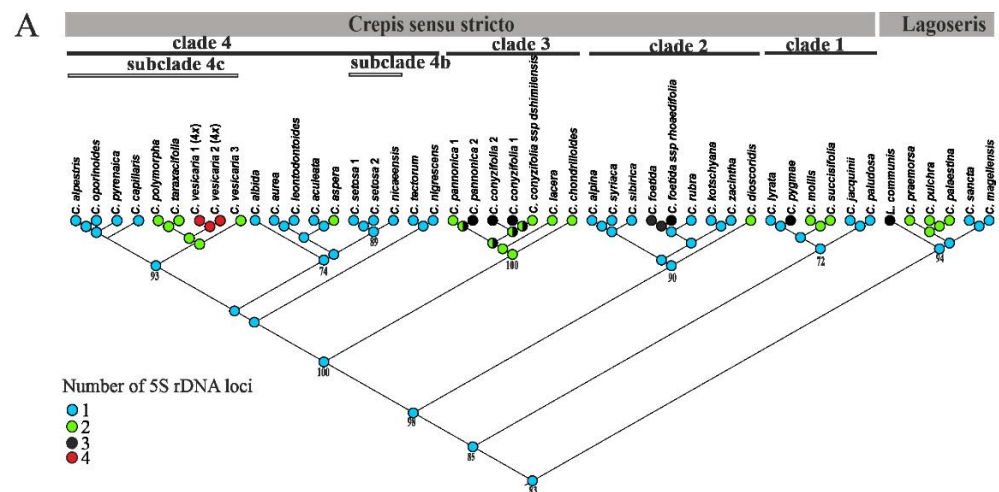


Figure 7. Cont.

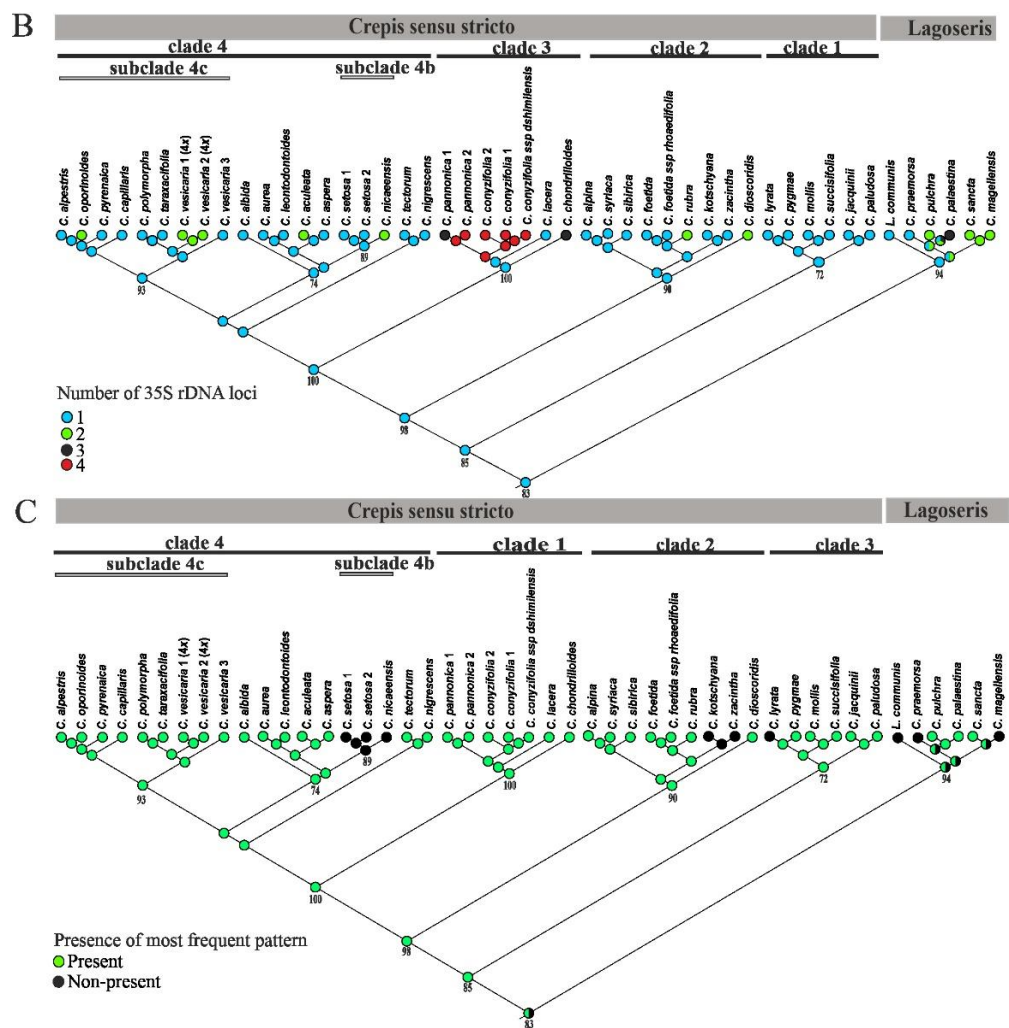


Figure 7. Ancestral character state reconstruction of the rDNA locus number and localisation for *Crepis* s.l. The numbers and localisation of the rDNA loci were mapped onto the ML tree of the nrITS sequences using maximum likelihood methods. (A) Number of 5S rDNA loci. (B) Number of 35S rDNA. (C) Presence/absence of the chromosome carrying both 35S and 5S rDNA loci within the same arm.

3. Discussion

Understanding the phylogenetic relationships between organisms is a prerequisite for almost any evolutionary study. Previous analyses of *Crepis* phylogeny revealed incongruences between the plastid and nrITS-based phylogenies [26,27]. The phylogenetic relationships that were inferred from the 5S rDNA NTS analyses were largely congruent with the nrITS-based phylogeny for the *Lagoseris* lineage but less so for the *Crepis* s.s. species. In the latter lineage, only a few basal nodes had good support. Nevertheless, the groups of closely related species that were recovered from analyses of both nuclear rDNA markers were largely congruent with previous studies [26,27]. The species with $x = 6$ (Table 1) that were monophyletic in the nrITS phylogeny were recovered in three well-supported clades (clades A, B and C) in the 5S rDNA NTS analysis.

Well-supported clade D, which primarily comprises perennial species that are related to the *C. conyzifolia* recovered in clade 3 in the ITS-based phylogeny, additionally included the annual *C. dioscoridis* in the 5S rDNA NTS-based phylogeny, which was similar to the cpDNA phylogeny [27]. This close relationship of *C. dioscoridis* to other species of clade D was also supported by cytogenetic analyses of the karyotype formula and rDNA loci distribution. Clades F and J corresponded to clade 2 in their ITS phylogeny, whereas clades E G, H, I and K corresponded to clade 4.

Unlike nrITS, which often showed genomic uniformity, 5S rDNA NTS sequences were usually highly polymorphic within individuals due to the absence of interlocus homogenisation [34]. The 5S rDNA NTS of different arrays had the potential to evolve independently. This may have led to multiple gene families in some diploid, as well as polyploid, plant species [35–37]. Despite this limitation, 5S rDNA NTS has been found to be very informative both at the intergeneric and at the species levels in many taxonomical groups (e.g., Refs. [38–40]), but there are also genera where this marker does not yield high resolution at either level [41]. Most of the species had only one dominant type of the 5S rDNA NTS variant, which is similar, as has previously been shown for many diploid species [42], although some intraindividual variations in the NTS region were recovered in some species. More than one type of 5S rDNA NTS were observed in some species that had more than one locus of 5S rDNA (Figures 1 and 2). Several reasons for such heterogeneity of 5S rDNA in diploids have been proposed, including an inefficient interlocus recombination that leads to a poor homogenisation or introgression [42,43].

The current study provided novel data on the 5S and 35S rDNA loci localisation for 38 species of *Crepis* and *L. communis*. Most of the analysed species had one locus of 35S rDNA in a subterminal chromosomal position and one interstitial 5S rDNA locus, which is an arrangement that is typical for many eudicots [44], including some taxa of the Asteraceae family, e.g., *Lactuca* [45], or species from the tribe Hieraciinae [34]. A quite characteristic feature of the karyotypes of most *Crepis* species was the presence of one chromosome that carried one of each 35S and 5S rDNA in one, usually short arm, with a 35S rDNA locus in the more distal and the 5S rDNA locus in the more proximal positions relative to one another. Although such an arrangement of rDNA loci is relatively rare among angiosperm species that have a single locus of each rDNA [44,46], in *Crepis*, this pattern has often been observed in karyotypes with either a single locus or multiple loci of rDNAs. Moreover, earlier reports on *Crepis* species revealed a similar arrangement of rDNA [30–32].

The interpretation of the rDNA loci distribution patterns in a phylogenetic context not only enables a better understanding of their evolution but also provides an insight into the evolution of the whole karyotype structure [21–23]. The most common reconstructed ancestral character state was the presence of a chromosome with both rDNA loci in one arm in the *Crepis* karyotype. Generally, the ancestral state of the rDNA loci number for *Crepis* s.l., but, also, for both lineages *Lagoseris* and *Crepis* s.s. was reconstructed as one locus of each 35S and 5S rDNA (Figure 8 and Supplementary Figure S4). Most of the analysed *Crepis* species had a larger number of rDNA loci, and relatively high interspecific polymorphisms in rDNA loci chromosomal organisation were observed. High variability in the number and localisation of rDNA loci were reported in many different plant genera, and usually, a higher polymorphism of the 35S rDNA locus number and distribution is common in plants [47–49]. The numbers of the increases in the 5S and 35S rDNA loci were quite similar in the analysed *Crepis* species, and the observed polymorphisms in the number and localisation of both rDNA loci were also comparable. The differences in the number and localisation of rDNA loci in related species have been assigned to various mechanisms, e.g., chromosomal rearrangements such as locus duplication/deletion and transposon-mediated transposition events [50–54]. The coding regions of rDNA sequences are an evolutionary very conserved fraction in the eucaryotic genome. This conservatism, however, appears to be a powerful source for genome instability, because the chromosomes that carry rDNA arrays (especially in subtelomeric regions) may be subject to unequal recombination and recombination between nonhomologous loci [55,56].

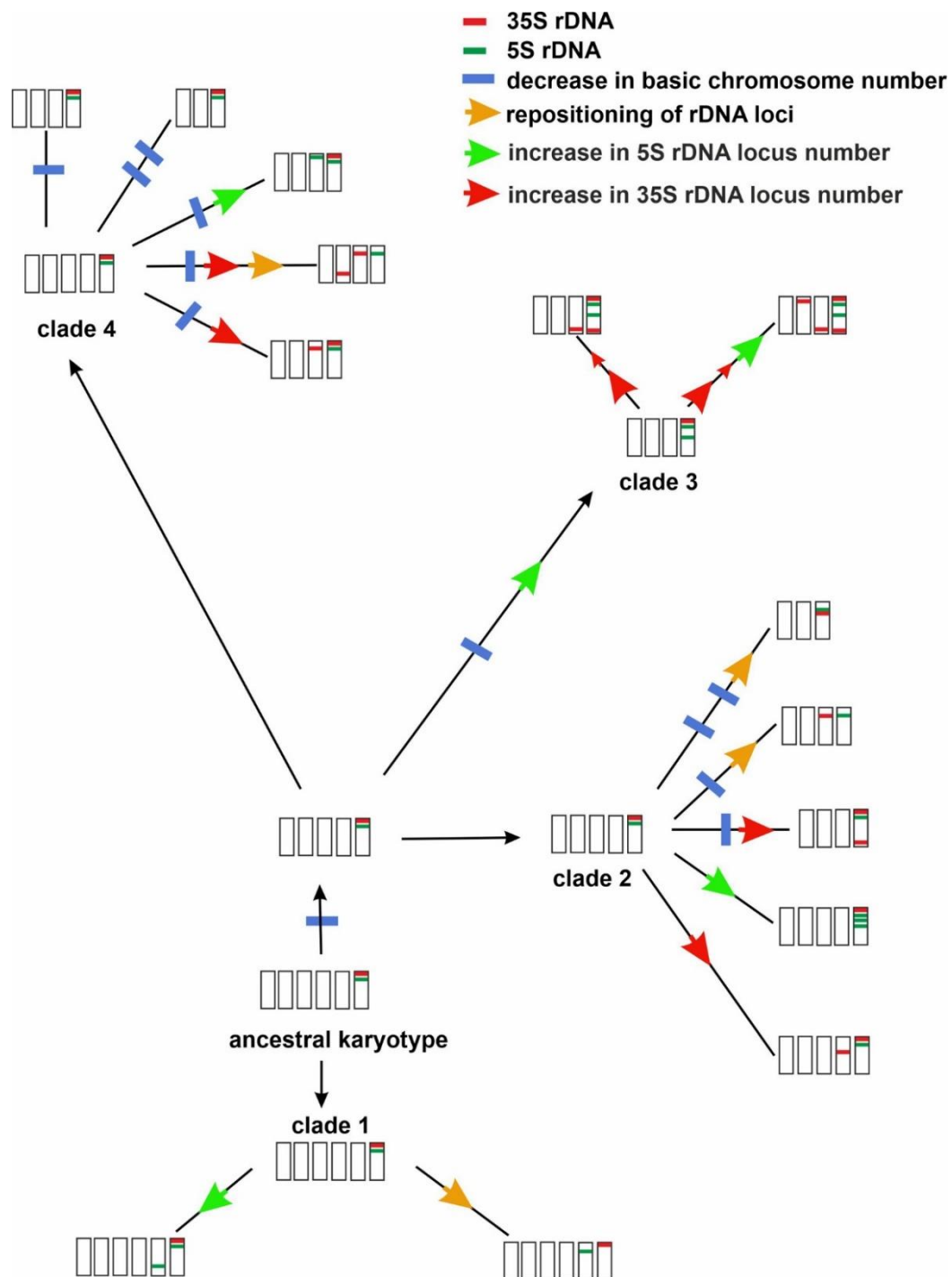


Figure 8. Hypothesis on the evolution of base chromosome numbers and rDNA loci number and localisation in *Crepis* s.s.

The ancestral state of the presence/absence of the chromosome carrying both rDNA locus types in one chromosome arm could not be unambiguously inferred for the *Lagoseris* lineage. Two or three events of rDNA loci repositioning explained their distribution patterns in extant species of this lineage. The repositioning of the rDNA loci has usually not been inferred for the same branches for which the changes in the base chromosome numbers in *Lagoseris* were inferred (Figure S5 [27]).

The common ancestor of the *Crepis* s.s. lineage was inferred to have had $x = 6$ and one locus of each of 35S and 5S rDNA in the same chromosomal arm with the 35S rDNA locus in a more distal position (Figures 8 and S5).

Most species of clade 1 had such a chromosome in their karyotype, and only one event of rDNA loci repositioning was inferred (the locus of the 35S rDNA and 5S rDNA in separate chromosomes). 5S rDNA loci gains were inferred for the evolution of three species in this clade. The evolution of the common ancestor of the species from clades 2, 3 and 4 accompanied a descending dysploidy (from $x = 6$ to $x = 5$). Further changes in the base chromosome number (from $x = 5$ to $x = 4$ and from $x = 4$ to $x = 3$), as well as both repositioning and gains of the rDNA loci, were reconstructed for the diversification and speciation of the taxa from clade 2 (Figure 8). The loci repositioning and descending dysploidy were supported in the same lineages, whereas the gains in the 35S rDNA loci numbers were inferred in lineages with a base chromosome number of $x = 5$ or $x = 4$, and the gain of 5S rDNA locus was inferred for line with $x = 5$ (Figures 8 and S5). The evolution of the common ancestor of clade 3 was accompanied by descending dysploidy and a gain of the 5S rDNA loci. Recently published data on genome size evolution in *Crepis* has also revealed a relatively large genome size increase during the evolution of this clade [27] that encompasses species with $x = 4$ exclusively. The further diversification in this clade was accompanied by a few events of rDNA loci gains and, as was earlier shown [27], increases in the genome size. However, it should be emphasised that the increases in genome size are primarily due to retrotransposons amplification in the plant [57], and the strong correlation between the increase in the number of rDNA loci and increases in genome size has not been described in plants [22,58,59]. Two species from this clade revealed relatively high intraspecific polymorphisms in rDNA loci chromosomal distribution. Silva et al. [60] showed that the amplification of repetitive sequences, mostly LTR retrotransposons, may shape the karyotype structure, promoting chromosome rearranging and changes in the chromosomal distribution of tandem repeats.

Clade 4, which is the most species-rich group of *Crepis* s.s., consists of species with base chromosome numbers of $x = 5, 4$ and 3. Its ancestral karyotype was reconstructed as having $x = 5$ and one locus of each 35S and 5S rDNA within the same chromosomal arm. Five events of subsequent descending dysploidy were inferred for this clade. One of these was reconstructed for the same lineage in which rDNA loci repositioning has occurred (subclade 4c). Three events of 5S rDNA loci gains and three events of 35S rDNA loci gains were inferred for this clade albeit in different lineages. Some events of descending dysploidy were inferred for the same lines in which increases of rDNA loci occurred (Figures 8 and S5). rDNA loci chromosomal distribution was, in many taxa, used as a cytotaxonomic character that allows grouping phylogenetically related species [58,61,62]. On the contrary, most clades distinguished in *Crepis* s.l. contained species that showed various patterns of rDNA loci distribution, as well as chromosome number, karyotype formula and genome size [27], except for clade 3, which included only species with $x = 5$ and similar karyotype formula. A common tendency to increase genome size and rDNA loci number was also inferred for this clade [27]. High polymorphisms in rDNA loci distribution were observed also in *Prospero*, *Chenopodium* s.l., *Brassica* and many other genera [21,22,63].

The translocation of the 35S rDNA locus to a different chromosome could explain the variations that were observed in species that did not have the chromosome with both types of rDNA loci in the same chromosomal arm. However, other mechanisms such as transposon-mediated transposition or minor locus amplification/major locus reduction cannot be excluded [52,64,65]. Inversions, which often accompany karyotype evolution in plants [66], might have been involved in the rearrangement of the two types of rDNA loci that were observed in *C. zacintha* (Figure 8). The evolution of clade 3, which has quite variable patterns of rDNA loci distribution, is accompanied by increases in the genome size [27]. An increase in genome size has often been shown to be caused by the activation and/or amplification of the retrotransposons [67,68], which might also mediate rDNA loci repatterning [52,69,70]. However, other mechanisms such as the chromosomal rearrangements

that are caused by unequal or ectopic recombination have also been postulated to play a role in karyotype rearrangements [51,52,64,65,71]. To gain a better understanding of the karyotype evolution in *Crepis*, comprehensive comparative analyses of repeatomes among *Crepis* species should be conducted. Such analyses not only will deliver new chromosomal markers but also give insight into mechanisms of genome size evolution in this taxon.

4. Materials and Methods

4.1. Plant Material and DNA Isolation

Forty-six accessions representing 39 *Crepis* species and *Lapsana communis* L. were used for the cytogenetic and molecular phylogenetic analyses. The plants were grown from seeds in a greenhouse facility of the University of Silesia under a 16 h/8 h photoperiod at 19 ± 2 °C. Vouchers were deposited at the Herbarium KTU (University of Silesia, Chorzów, Poland; Table 2). Total genomic DNA was isolated from fresh leaf tissue using the modified CTAB method [72]. Genomic DNAs were analysed for quality and quantity using a NanoDrop™ spectrophotometer (ND-1000, peqLab, Erlangen, Germany). The 5S rDNA NTS sequences were amplified from the same DNA extracts as the nrITS that were reported by Senderowicz et al. [27]. The FISH results were obtained for five to ten individuals per accession, except for *C. chondrilloides* (two individuals) and *C. nigrescens* (three individuals), and always included the individuals that had been used for the DNA extraction.

Table 2. Species name, collection number and voucher number of the analysed taxa and GenBank accession numbers of the sequences obtained in this research.

Species	Collection Number	Voucher Number	5S rDNA NTS
			GenBank Number
<i>Crepis</i> s.s.			
<i>Crepis aculeata</i> Boiss.	BGT 38	KTU154623	MZ226690–MZ226694
<i>C. albida</i> Vill.	UGA 233	-	MZ226725–MZ226729
<i>C. alpestris</i> (Jacq.) Tausch	BGUG N49	KTU157712	MZ226695–MZ226699
<i>C. alpina</i> L.	USDA PI 274367	KTU154609	MZ226705–MZ226709
<i>C. aspera</i> L.	LBG 006722	KTU157716	MZ226715–MZ226719
<i>C. aurea</i> (L.) Cass.	USDA PI 312843	KTU157719	MZ226720–MZ226724
<i>C. capillaris</i> Wallr.	BGGU 335	KTU154610	MZ226735–MZ226739
<i>C. conyzifolia</i> (Gouan) A.Kern. (1)	GBA 462	KTU157720	MZ226740–MZ226744
<i>C. conyzifolia</i> (Gouan) A.Kern. (2)	UGA 236	-	MZ226745–MZ226749
<i>C. conyzifolia</i> subsp. <i>dshimilensis</i> (K.Koch) Lamond (3)	GBBG	-	MZ226839–MZ226843
<i>C. chondrilloides</i> Jacq.	Triest, Italy 45°36'46.54" N 13°51'36.96" E	-	MZ226952–MZ226956

Table 2. Cont.

Species	Collection Number	Voucher Number	5S rDNA NTS
			GenBank Number
<i>C. dioscoridis</i> L.	IPK CRE2	KTU154619	MZ226750–MZ226754
<i>C. foetida</i> L.	USDA PI 296071	KTU154612	MZ226755–MZ226759
<i>C. foetida</i> subsp. <i>rhoaedifolia</i> (M.Bieb.) Celak.	HBBH 1734	KTU154614	MZ226864–MZ226868
<i>C. jacquinii</i> Tausch	Sarnia Skała Tatra Mts, Poland 49°15'52.77" N 19°56'30.36" E	KTU159736	MZ226760–MZ226764
<i>C. kotschyana</i> Boiss.	USDA PI 310392	KTU164608	MZ226765–MZ226769
<i>C. lacera</i> Ten.	BGMN	KTU159735	MZ226770–MZ226774
<i>C. leontodontoides</i> All.	BGDG 658	KTU154631	MZ226775–MZ226779
<i>C. lyrata</i> (L.) Froel.	SSBG	-	MZ226780–MZ226785
<i>C. mollis</i> Asch.	Sławków, Poland 50°17'45.90" N 19°16'59.06" E	KTU154630	MZ226792–MZ226796
<i>C. nicaeensis</i> Balb.	BGEU	KTU157730	MZ226797–MZ226801
<i>C. nigrescens</i> Pohle	HUM	-	MZ226802–MZ226806
<i>C. oporinoides</i> Boiss. ex Froel.	ABGL 1516	KTU154622	MZ226710–MZ226714
<i>C. paludosa</i> Moench	Sławków, Poland 50°18'07.51" N 19°21'19.10" E	KTU154625	MZ226807–MZ226811
<i>C. pannonica</i> (Jacq.) K.Koch (1)	BGBD 256-01-00-14	KTU154627	MZ226817–MZ226826
<i>C. pannonica</i> (Jacq.) K.Koch (2)	BGEU	KTU157729	MZ226827–MZ226833
<i>C. polymorpha</i> Pourr	JBN 149	KTU157725	MZ226834–MZ226838
<i>C. pygmaea</i> L.	UGA 239	KTU157722	MZ226854–MZ226858
<i>C. pyrenaica</i> (L.) Greuter	BGBD 1010	KTU154621	MZ226859–MZ226863
<i>C. rubra</i> L.	BGK 364	KTU154607	MZ226869–MZ226873
<i>C. setosa</i> Haller f. 1	HBUR 1275	KTU154620	MZ226879–MZ226883
<i>C. sibirica</i> L.	BGBD 738	KTU157721	MZ226884–MZ226889
<i>C. succisifolia</i> Tausch	Redziny, Poland 50°49'08.66" N 15°55'55.27" E	KTU154656	MZ226890–MZ226894

Table 2. Cont.

Species	Collection Number	Voucher Number	5S rDNA NTS
			GenBank Number
<i>C. syriaca</i> (Bornm.) Bab. & Navashin	KEW 0129064	KTU154615	MZ226895–MZ226899
<i>C. taraxacifolia</i> Thuill.	BGGU 347	KTU157723	MZ226900–MZ226904
<i>C. tectorum</i> L.	Ustroń, Poland 49°43'14.68" N 18°49'29.11" E	KTU157717	MZ226905–MZ226909
<i>C. veiscaria</i> L. 1 (4x)	BGBD 1014	KTU154616	MZ226910–MZ226920
<i>C. vesicaria</i> L. 2 (4x)	BGBD 918	KTU157726	MZ226921–MZ226931
<i>C. vesicaria</i> L. 3 (2x)	OBUP	KTU157724	MZ226932–MZ226936
<i>C. zacintha</i> (L.) Loisel.	BGT 92	KTU154606	MZ226937–MZ226941
Lagoseris			
<i>C. magellensis</i> F. Conti & Uzunov	BGMN	KTU157727	MZ226787–MZ226791
<i>C. palaestina</i> Bornm.	BGGU 335	KTU154611	MZ226812–MZ226816
<i>C. pulchra</i> L.	BGGU 341	KTU154648	MZ226849–MZ226853
<i>C. preamorsa</i> (L.) Tausch	BGBD 662	KTU154628	MZ226844–MZ226848
<i>C. sancta</i> (L.) Bornm.	BGUK 104	KTU154613	MZ226874–MZ226878
<i>Lapsana communis</i> L.	KEW 0018568	KTU154617	MZ226942–MZ226946
Outgroup			
<i>Picris hieracioides</i> L.	Jaworzno Poland 50°13'31.43" N 19°16'28.63" E	KTU157710	MZ226947–MZ226951

Voucher deposited in KTU; seed origin and accession number: (BGT) Botanic Garden of Tel Aviv University; (USDA) USDA North Central Regional Plant Introduction Station of the US National Plant Germplasm System; (UGA) Université Grenoble Alpes; (JBI) Jardín Botánico de Iturraran Lorategi Botanikoa, Spain; (BGUG) Botanical Garden of Universität Graz; (BGBD) Botanical Garden Freie Universität Berlin—Dahlem; (LBG) Lyon Botanical Garden, France; (WB) Wolosate, Bieszczady National Park, Poland; (BGGU) The Botanical Garden of Göttingen University; (GBA) Giardino Botanico Alpino “Rezia”, Italy; (GBBG) Gruzja Batumi Botanical Garden; (IPK) The Leibniz Institute of Plant Genetics and Crop Plant Research (IPK), Germany; (HBBH) Hortus Botanicus Budapest, Hungary; (BGMN) Botanical Gardens of Majella National Park, Italy; (SSBG) The South-Siberian Botanical Garden of Altai State University; (BGEU) Botanical Garden of Eötvös University in Budapest; (HUM) Herbarium Universitatis Mosquensis; (ABGL) Alpine Botanical Garden of Lautaret, France; (JBN) Jardin Botanique de Nancy; (BGK) Botanical Garden in Kiel; (HBUR) Hortus Botanicus Universitatis, Romania; (KEW) Millennium Seed Bank KEW Gardens; (OBUP) Orto Botanico Dell Università Di Padova Italia; (BGUK) Botanischer Garten Universität Konstanz, Germany.

4.2. DNA Amplification and Sequencing

The internal transcribed spacers of the 35S rRNA gene (nrITS, including ITS1, the intervening 5.8S rDNA and ITS2) were amplified from the *C. chondrilloides* genome using a primer pair anchored in 18S rDNA and 25S rDNA (18S dir [5'-CGTAACAAGGTTTCCGTAGG-3'] and 25S com [5'-AGCGGGTAGTCCCCGCCTGA-3'], as was published earlier [27,73]. The nucleotide sequence of nrITS isolated from *C. chondrilloides* is available in GenBank under

number MZ226957. All of the other nrITS sequence data were obtained from GenBank (Supplementary Table S1).

The 5S rDNA non-transcribed spacer (5S rDNA NTS) region was amplified from the genomic DNAs that had been isolated from 45 accessions of *Crepis*, one accession of *Lapsana communis* and one accession of *Picris hieracioides*, which was used as an outgroup. The PCR amplification of the 5S rDNA NTS and the cloning of this region were performed according to Kolano et al. [74]. Positive colonies were transferred into clean Eppendorf tubes (1.5 mL), dissolved in 100 µL of ddH₂O, incubated for 10 min at 96 °C and cooled down on ice for 10 min. These samples served as the DNA template for the PCR reactions using the M13 primers. The reactions were performed using Taq DNA Polymerase from *Thermus aquaticus* (SIGMA, St. Louis, MO, USA) according to the manufacturer's instructions. The PCR amplification protocol consisted of an initial denaturation step of 2 min at 94 °C, followed by 35 cycles of amplification consisting of 40 s denaturation at 94 °C, 40 s of primer annealing at 55 °C and 40 s of DNA extension at 72 °C. All of the PCR products were treated with *E. coli* Exonuclease I and FastAP Termosensitive Alkaline Phosphatase (Thermo Fisher Scientific, Waltham, MA, USA) according to the manufacturer's instructions. The product sequencing was performed by Macrogen (Amsterdam, The Netherlands) using a 3730xl DNA Analyser (Applied Biosystems, Foster City, CA, USA). At least five clones were analysed for each diploid accession and ten clones for each tetraploid accession. All of the sequences were deposited in GenBank (the accession numbers are listed in Table 2).

4.3. Phylogenetic Analyses, Inferences of the Patterns of the Evolution of the rDNA Loci and Ancestral State Reconstructions

Phylogenetic analyses were performed using the DNA sequences of 5S rDNA NTS and the nrITS regions obtained in this study and those published earlier (Supplementary Table S1 [27]), which represent multiple species of two evolutionary lineages of the genus *Lagoseris* and *Crepis* s.s. Multiple sequence alignments for both datasets were performed 20 times using webPRANK [75] and MergeAlign [76] in order to obtain a consensus multiple sequence alignment. The phylogenetic relationships were inferred using maximum likelihood (ML) analyses as implemented in IQ-TREE version 0.9.5 [77]. *Picris hieracioides*, *Lactuca seriola* and *Sonchus oleraceus* were used as the outgroup taxa. The ITS dataset comprised all of the studied species. The 5S rDNA NTS sequences were too variable to obtain a reliable alignment in the phylogenetic analyses. Therefore, the analyses were performed separately for the *Lagoseris* and *Crepis* s.s. evolutionary lineages. The significance of the inferred relationships was assessed via bootstrapping with 1000 replicates. The most appropriate model of sequence evolution for the ML analyses was determined using the Bayesian information criterion as implemented in IQ-TREE. The best-fit model that was selected for the nrITS was TIM3e + G4. For analyses of the 5S rDNA NTS, the best-fit models were K2P + G4 for *Lagoseris* (rooted with *Picris hieracioides*) and K3P + G4 for *Crepis* s.s. lineage (rooted with *C. praemorsa*).

The phylogram that resulted from the ML analysis was used to infer the evolution of the chromosomal organisation of the rDNA loci and base chromosome number. The analyses were performed using the better-supported nrITS phylogram. Three characters were analysed separately: (i) the number of 5S rDNA loci, (ii) the number of 35S rDNA loci and (iii) the presence/absence of the chromosome carrying both the 5S and 35S rDNA loci within the same arm. The analysis was performed using the ML method as implemented in Mesquite [78]. The nrITS phylogram was also used to infer the evolution of the base chromosome numbers with ChromEvol. The maximum likelihood analysis was performed under the CONST_RATE model as implemented in ChromEvol 2.0. software [79]. For the ChromEvol analyses, the best-fit model was tested using an AIC test (Table S2). For the best-fitted model, the analyses were rerun with parameters that were fixed to those that were optimised in the first run using 10,000 simulations to compute the expected number of changes along each branch, as well as the ancestral haploid chromosome numbers at the nodes.

4.4. Chromosome Preparation and Fluorescent In Situ Hybridisation

Young leaves were used as the material to prepare the chromosomal spreads. The leaves were pre-treated with 2-mM 8-hydroxyquinoline for 2 h at room temperature and 2 h at 4 °C, fixed in methanol:glacial acetic (3:1) and stored at −20 °C until they were used. The mitotic metaphase chromosome spreads were prepared according to Dydak et al. [80] using an enzyme mixture consisting of 20% pectinase (SIGMA, St. Louis, MO, USA) and 4% cellulose (Onozuka R-10; Serva, Heidelberg, Germany). The coding region of the 25S rRNA that was isolated from *Arabidopsis thaliana* [81] and labelled with rhodamine-4-dUTP (Roche, Basel, Switzerland) was used to detect the 35S rDNA loci. The 5S rDNA monomer that was isolated from *Triticum aestivum* [82] and labelled with digoxigenin-11-dUTP (Roche, Basel, Switzerland) was used to detect the 5S rDNA loci. Both probes were labelled using nick translation according to manufacturer's instructions (Roche, Basel, Switzerland). FISH was performed according to Kolano et al. [74]. The hybridisation mixture consisting of 100 ng of each labelled DNA probe, 50% formamide, 2 × SSC and 10% dextran sulphate was denatured for 10 min at 95 °C and immediately cooled down on ice. The denaturation of the slides and the hybridisation mixture were performed on an Omnislide Thermal cycler (ThermoHybaid, Franklin, MA, USA) at 72 °C for 4 min. Hybridisation was conducted for 48 h at 37 °C in a humid chamber. Stringent washes (0.1 × SSC at 42 °C) were followed by the detection of digoxigenin using the FITC-conjugated primary anti-digoxigenin antibody (Roche, Basel, Switzerland). The signals were then amplified using secondary FITC-conjugated anti-sheep antibodies (Jackson ImmunoResearch, West Grove, PA, USA). The slides were analysed under a Zeiss AxioImager.Z.2 fluorescence microscope (Zeiss, Aalen, Germany); the images were acquired with an AxioCam HMr camera attached to an AxioImager.Z.2 wide-field epifluorescence microscope (both Zeiss, Oberkochen, Germany) and processed uniformly using ZEN 2.3 Pro (Zeiss) and Photoshop CS3 (Adobe, San Jose, CA, USA).

4.5. Fluorochrome Banding

The chromosomal spreads that were used for CMA3 banding were prepared according to Dydak et al. [80]. Double-fluorescence staining with chromomycin A₃ (CMA₃) and 4',6-diamidino-2-phenylindole (DAPI) was performed as described by Kolano et al. [83]. The slides were analysed with an Olympus PROVIS AX70 fluorescence microscope (Olympus, Tokyo, Japan), and the images were acquired with a Retiga-2000R Fast1394 camera (QImaging, Surrey, BC, Canada).

5. Conclusions

The patterns of the number and localisation of the 5S and 35S rDNA loci in *Crepis* species revealed an interspecific variation. Some of these characters were shared by most of the analysed species, notably the presence of a chromosome that carried both the 35S and 5S rDNA loci within the same arm. A hypothetical ancestral karyotype of *Crepis* s.l. was reconstructed as having one locus of each 5S and 35S rDNA. The common ancestor of *Crepis* s.s. carried these two rDNA locus types in one chromosomal arm. Several events of both 35S and 5S rDNA loci repatterning, which involved the repositioning of the loci and a change of their numbers, were inferred to have accompanied the evolution of the rDNA loci. Some of the changes in rDNA loci repatterning seem to coincide with descending dysploidy. This study provides the first comprehensive in-depth analysis of the karyotypes of numerous *Crepis* species beyond their chromosome numbers and karyotype structures. It should serve as the basis for more detailed analyses of the *Crepis* genomes using more chromosomal markers that represent various repetitive DNA families.

Supplementary Materials: The following supporting information can be downloaded at <https://www.mdpi.com/article/10.3390/ijms23073643/s1>.

Author Contributions: B.K. conceived and designed the study; M.S. performed the laboratory work; M.S. and B.K. performed the subsequent data analyses; T.N. and L.P. collected the plant material and B.K., H.W.-S. and M.S., writing—original draft preparation. All authors have read and agreed to the published version of the manuscript.

Funding: This research was funded by the National Science Centre, Poland (Project No. 2017/27/B/NZ8/01478).

Institutional Review Board Statement: Not applicable.

Informed Consent Statement: Not applicable.

Data Availability Statement: The nucleotide sequences are available in GenBank (<http://www.ncbi.nlm.nih.gov/genbank>, accessed on 28 February 2022) under numbers MZ226695–MZ226956 and MZ226957. Other data generated or analysed during this study are available from the corresponding author upon reasonable request.

Conflicts of Interest: The authors declare no conflict of interest.

References

- Li, S.-F.; Su, T.; Cheng, G.-Q.; Wang, B.-X.; Li, X.; Deng, C.-L.; Gao, W.-J. Chromosome evolution in connection with repetitive sequences and epigenetics in plants. *Genes* **2017**, *8*, 290. [[CrossRef](#)] [[PubMed](#)]
- Schubert, I.; Vu, G.T.H. Genome stability and evolution: Attempting a holistic view. *Trends Plant Sci.* **2016**, *21*, 749–757. [[CrossRef](#)] [[PubMed](#)]
- Sancho, R.; Inda, L.A.; Díaz-Pérez, A.; Des Marais, D.L.; Gordon, S.; Vogel, J.; Lusinska, J.; Hasterok, R.; Contreras-Moreira, B.; Catalán, P. Tracking the ancestry of known and ‘Ghost’ homeologous subgenomes in model grass *Brachypodium* polyploids. *Plant J.* **2022**. [[CrossRef](#)] [[PubMed](#)]
- Mandáková, T.; Guo, X.; Özüdoğru, B.; Mummenhoff, K.; Lysak, M.A. Hybridization-facilitated genome merger and repeated chromosome fusion after 8 million years. *Plant J.* **2018**, *96*, 748–760. [[CrossRef](#)]
- Mota, L.; Torices, R.; Loureiro, J. The evolution of haploid chromosome numbers in the sunflower family. *Genome Biol. Evol.* **2016**, *8*, 3516–3528. [[CrossRef](#)]
- Ferraz, M.E.; Fonsêca, A.; Pedrosa-Harand, A. Multiple and independent rearrangements revealed by comparative cytogenetic mapping in the dysploid *Leptostachyus* group (*Phaseolus* L., Leguminosae). *Chromosome Res.* **2020**, *28*, 395–405. [[CrossRef](#)]
- Lusinska, J.; Betekhtin, A.; Lopez-Alvarez, D.; Catalan, P.; Jenkins, G.; Wolny, E.; Hasterok, R. Comparatively barcoded chromosomes of *Brachypodium* perennials tell the story of their karyotype structure and evolution. *Int. J. Mol. Sci.* **2019**, *20*, 5557. [[CrossRef](#)]
- Lusinska, J.; Majka, J.; Betekhtin, A.; Susek, K.; Wolny, E.; Hasterok, R. Chromosome identification and reconstruction of evolutionary rearrangements in *Brachypodium distachyon*, *B. stacei* and *B. hybridum*. *Ann. Bot.* **2018**, *122*, 445–459. [[CrossRef](#)]
- Liu, X.; Sun, S.; Wu, Y.; Zhou, Y.; Gu, S.; Yu, H.; Yi, C.; Gu, M.; Jang, J.; Liu, B.; et al. Dual-color oligo-FISH can reveal chromosomal variations and evolution in *Oryza* species. *Plant J.* **2020**, *101*, 112–121. [[CrossRef](#)]
- Lysak, M.A.; Mandáková, T.; Schranz, M.E. Comparative paleogenomics of crucifers: Ancestral genomic blocks revisited. *Curr. Opin. Plant Biol.* **2016**, *30*, 108–115. [[CrossRef](#)]
- Mandaáková, T.; Lysak, M.A. Chromosomal phylogeny and karyotype evolution in $x=7$ crucifer species (Brassicaceae). *Plant Cell* **2008**, *20*, 2559–2570. [[CrossRef](#)] [[PubMed](#)]
- Mandáková, T.; Lysak, M.A. Post-polyloid diploidization and diversification through dysploid changes. *Curr. Opin. Plant Biol.* **2018**, *42*, 55–65. [[CrossRef](#)] [[PubMed](#)]
- Braz, G.T.; He, L.; Zhao, H.; Zhang, T.; Semrau, K.; Rouillard, J.M.; Torres, G.A.; Jiang, J. Comparative oligo-FISH mapping: An efficient and powerful methodology to reveal karyotypic and chromosomal evolution. *Genetics* **2018**, *208*, 513–523. [[CrossRef](#)] [[PubMed](#)]
- Jiang, J. Fluorescence in situ hybridization in plants: Recent developments and future applications. *Chromosome Res.* **2019**, *27*, 153–165. [[CrossRef](#)]
- Lee, Y.-I.; Yap, J.W.; Izan, S.; Leitch, I.J.; Fay, M.F.; Lee, Y.-C.; Hidalgo, O.; Dodsworth, S.; Smulders, M.J.M.; Gravendeel, B.; et al. Satellite DNA in *Paphiopedilum* subgenus *Parvisepalum* as revealed by high-throughput sequencing and fluorescent in situ hybridization. *BMC Genom.* **2018**, *19*, 578. [[CrossRef](#)]
- Waminal, N.E.; Pellerin, R.J.; Kang, S.-H.; Kim, H.H. Chromosomal mapping of tandem repeats revealed massive chromosomal rearrangements and insights into *Senna tora* dysploidy. *Front. Plant Sci.* **2021**, *12*, 629898. [[CrossRef](#)]
- Moraes, A.P.; Olmos Simões, A.; Ojeda Alayon, D.I.; de Barros, F.; Forni-Martins, E.R. Detecting mechanisms of karyotype evolution in *Heterotaxis* (Orchidaceae). *PLoS ONE* **2016**, *11*, e0165960. [[CrossRef](#)]
- Costa, L.; Oliveira, Á.; Carvalho-Sobrinho, J.; Souza, G. Comparative cytomechanical analyses reveal karyotype variability related to biogeographic and species richness patterns in Bombacoideae (Malvaceae). *Plant Syst. Evol.* **2017**, *303*, 1131–1144. [[CrossRef](#)]

19. Volkov, R.; Medina, F.; Zentgraf, U.; Hemleben, V. Organization and molecular evolution of rDNA nucleolar dominance and nucleolus structure. In *Progress in Botany*; Esser, K., Lutge, U., Beyschlag, W., Murata, J., Eds.; Springer: Berlin/Heidelberg, Germany; New York, NY, USA, 2004; Volume 65.
20. Vasconcelos, E.V.; Vasconcelos, S.; Ribeiro, T.; Benko-Iseppon, A.M.; Brasileiro-Vidal, A.C. Karyotype heterogeneity in *Philodendron* s.l. (Araceae) revealed by chromosome mapping of rDNA loci. *PLoS ONE* **2018**, *13*, e0207318. [[CrossRef](#)]
21. Kolano, B.; Siwinska, D.; McCann, J.; Weiss-Schneeweiss, H. The evolution of genome size and rDNA in diploid species of *Chenopodium* s.l. (Amaranthaceae). *Bot. J. Linn. Soc.* **2015**, *179*, 218–235. [[CrossRef](#)]
22. Jang, T.-S.; Emadzade, K.; Parker, J.; Tensch, E.M.; Leitch, A.R.; Speta, F.; Weiss-Schneeweiss, H. Chromosomal diversification and karyotype evolution of diploids in the cytologically diverse genus *Prospero* (Hyacinthaceae). *BMC Evol. Biol.* **2013**, *13*, 136. [[CrossRef](#)] [[PubMed](#)]
23. Costa, L.; Jimenez, H.; Carvalho, R.; Carvalho-Sobrinho, J.; Escobar, I.; Souza, G. Divide to conquer: Evolutionary history of Alliioideae tribes (Amaryllidaceae) is linked to distinct trends of karyotype evolution. *Front. Plant Sci.* **2020**, *11*, 320. [[CrossRef](#)] [[PubMed](#)]
24. Feliner, G.N.; Rossello, J.A. Better the devil you know? Guidelines for insightful utilization of nrDNA ITS in species-level evolutionary studies in plants. *Mol. Phylogenet. Evol.* **2007**, *44*, 911–919. [[CrossRef](#)] [[PubMed](#)]
25. Garcia, S.; Panero, J.L.; Siroky, J.; Kovarik, A. Repeated reunions and splits feature the highly dynamic evolution of 5S and 35S ribosomal RNA genes (rDNA) in the Asteraceae family. *BMC Plant Biol.* **2010**, *10*, 176. [[CrossRef](#)] [[PubMed](#)]
26. Enke, N.; Gemeinholzer, B. Babcock revisited: New insights into generic delimitation and character evolution in *Crepis* L. (Compositae: Cichorieae) from ITS and *matK* sequence data. *Taxon* **2008**, *57*, 756–768. [[CrossRef](#)]
27. Senderowicz, M.; Nowak, T.; Rojek-Jelonek, M.; Bisaga, M.; Papp, L.; Weiss-Schneeweiss, H.; Kolano, B. Descending dysploidy and bidirectional changes in genome size accompanied *Crepis* (Asteraceae) evolution. *Genes* **2021**, *12*, 1436. [[CrossRef](#)]
28. Babcock, E.B. *The Genus Crepis I. The Taxonomy, Phylogeny, Distribution and Evolution of Crepis. The Genus Crepis II. Systematic Treatment*; University of California Press: Berkeley, CA, USA; Los Angeles, CA, USA, 1947.
29. Jamilena, M.; Ruiz Rejón, C.; Ruiz Rejón, M. Repetitive DNA sequence families in *Crepis capillaris*. *Chromosoma* **1993**, *102*, 272–278. [[CrossRef](#)]
30. Enke, N.; Kunze, R.; Pustahija, F.; Glöckner, G.; Zimmermann, J.; Oberländer, J.; Kamari, G.; Siljak-Yakovlev, S. Genome size shifts: Karyotype evolution in *Crepis* section *Neglectoides* (Asteraceae). *Plant Biol.* **2015**, *17*, 775–786. [[CrossRef](#)]
31. Maluszynska, J.; Schweizer, D. Ribosomal RNA genes in B chromosomes of *Crepis capillaris* detected by non-radioactive *in situ* hybridization. *Heredity* **1989**, *62*, 59–65. [[CrossRef](#)]
32. Hizume, M. Chromosomal localization of 5S rRNA genes in *Vicia faba* and *Crepis capillaris*. *Cytologia* **1993**, *58*, 417–421. [[CrossRef](#)]
33. Schweizer, D. Reverse fluorescent chromosome banding with chromomycin and DAPI. *Chromosoma* **1976**, *58*, 307–324. [[CrossRef](#)] [[PubMed](#)]
34. Fehrer, J.; Slavíková, R.; Paštová, L.; Josefiová, J.; Mráz, P.; Chrtek, J.; Bertrand, Y.J.K. Molecular evolution and organization of ribosomal DNA in the Hawkweed Tribe Hieraciinae (Cichorieae, Asteraceae). *Front. Plant Sci.* **2021**, *12*, 647375. [[CrossRef](#)] [[PubMed](#)]
35. Kolano, B.; McCann, J.A.M.I.E.; Oskędra, M.; Chrapek, M.; Rojek, M.; Nobis, A.; Weiss-Schneeweiss, H. Parental origin and genome evolution of several eurasian hexaploid species of chenopodium (Chenopodiaceae). *Phytotaxa* **2019**, *392*, 163–185. [[CrossRef](#)]
36. Volkov, R.A.; Panchuk, I.I.; Borisjuk, N.V.; Hosiawa-Baranska, M.; Maluszynska, J.; Hemleben, V. Evolutional dynamics of 45S and 5S ribosomal DNA in ancient allohexaploid *Atropa belladonna*. *BMC Plant Biol.* **2017**, *17*, 21. [[CrossRef](#)] [[PubMed](#)]
37. Matyáček, R.; Fulneček, J.; Lim, K.Y.; Leitch, A.R.; Kovarik, A. Evolution of 5S rDNA unit arrays in the plant genus *Nicotiana* (Solanaceae). *Genome* **2002**, *45*, 556–562. [[CrossRef](#)] [[PubMed](#)]
38. Persson, C. Phylogeny of the Neotropical *Alibertia* group (Rubiaceae), with emphasis on the genus *Alibertia*, inferred from ITS and 5S ribosomal DNA sequences. *Am. J. Bot.* **2000**, *87*, 1018–1028. [[CrossRef](#)] [[PubMed](#)]
39. Waminal, N.E.; Ryu, K.B.; Park, B.R.; Kim, H.H. Phylogeny of Cucurbitaceae species in Korea based on 5S rDNA non-transcribed spacer. *Genes Genom.* **2014**, *36*, 57–64. [[CrossRef](#)]
40. Grabiele, M.; Aguilera, P.M.; Ducasse, D.A.; Debat, H.J. Molecular characterization of the 5S rDNA non-Transcribed spacer and reconstruction of phylogenetic relationships in Capsicum. *Rodriguesia* **2021**, *72*. [[CrossRef](#)]
41. Pornpongrungrueng, P.; Borchsenius, F.; Gustafsson, M.H.G. Relationships within *Blumea* (Inuleae, Asteraceae) and the Utility of the 5S-NTS in Species-Level Phylogeny Reconstruction. *Taxon* **2009**, *58*, 1181–1193. [[CrossRef](#)]
42. Garcia, S.; Wendel, J.F.; Borowska-Zuchowska, N.; Ainouche, M.; Kuderova, A.; Kovarik, A. The utility of graph clustering of 5S ribosomal DNA homoeologs in plant allopolyploids, homoploid hybrids, and cryptic introgressants. *Front. Plant Sci.* **2020**, *11*, 41. [[CrossRef](#)]
43. Simon, L.; Rabanal, F.A.; Dubos, T.; Oliver, C.; Lauber, D.; Poulet, A.; Vogt, A.; Mandlbauer, A.; Le Goff, S.; Sommer, A.; et al. Genetic and epigenetic variation in 5S ribosomal RNA genes reveals genome dynamics in *Arabidopsis thaliana*. *Nucleic Acids Res.* **2018**, *46*, 3019–3033. [[CrossRef](#)] [[PubMed](#)]
44. Garcia, S.; Kovarik, A.; Leitch, A.R.; Garnatje, T. Cytogenetic features of rRNA genes across land plants: Analysis of the Plant rDNA database. *Plant J.* **2017**, *89*, 1020–1030. [[CrossRef](#)] [[PubMed](#)]

45. Matoba, H.; Mizutani, T.; Nagano, K.; Hoshi, Y.; Uchiyama, H. Chromosomal study of lettuce and its allied species (*Lactuca* spp., Asteraceae) by means of karyotype analysis and fluorescence in situ hybridization. *Hereditas* **2007**, *144*, 235–243. [[CrossRef](#)] [[PubMed](#)]
46. Roa, F.; Guerra, M. Non-random distribution of 5S rDNA sites and its association with 45S rDNA in plant chromosomes. *Cytogenet. Genome Res.* **2015**, *146*, 243–249. [[CrossRef](#)]
47. Clarkson, J.J.; Lim, K.Y.; Kovarik, A.; Chase, M.W.; Knapp, S.; Leitch, A.R. Long-term genome diploidization in allopolyploid *Nicotiana* section *Repandae* (Solanaceae). *New Phytol.* **2005**, *168*, 241–252. [[CrossRef](#)]
48. Jang, T.-S.; McCann, J.; Parker, J.S.; Takayama, K.; Hong, S.-P.; Schneeweiss, G.M.; Weiss-Schneeweiss, H. rDNA loci evolution in the genus *Glechoma* (Lamiaceae). *PLoS ONE* **2016**, *11*, e0167177. [[CrossRef](#)]
49. Książczyk, T.; Taciak, M.; Zwierzykowski, Z. Variability of ribosomal DNA sites in *Festuca pratensis*, *Lolium perenne*, and their intergeneric hybrids, revealed by FISH and GISH. *J. Appl. Genet.* **2010**, *51*, 449–460. [[CrossRef](#)]
50. Belyayev, A. Bursts of transposable elements as an evolutionary driving force. *J. Evol. Biol.* **2014**, *27*, 2573–2584. [[CrossRef](#)]
51. Kalendar, R.; Raskina, O.; Belyayev, A.; Schulman, A.H. Long tandem arrays of Cassandra retroelements and their role in genome dynamics in plants. *Int. J. Mol. Sci.* **2020**, *21*, 2931. [[CrossRef](#)]
52. Raskina, O.; Barber, J.C.; Nevo, E.; Belyayev, A. Repetitive DNA and chromosomal rearrangements: Speciation-related events in plant genomes. *Cytogenet. Genome Res.* **2008**, *120*, 351–357. [[CrossRef](#)]
53. Książczyk, T.; Zwierzykowska, E.; Molik, K.; Taciak, M.; Krajewski, P.; Zwierzykowski, Z. Genome-dependent chromosome dynamics in three successive generations of the allotetraploid *Festuca pratensis* × *Lolium perenne* hybrid. *Protoplasma* **2015**, *252*, 985–996. [[CrossRef](#)] [[PubMed](#)]
54. Thomas, H.M.; Harper, J.A.; Morgan, W.G. Gross chromosome rearrangements are occurring in an accession of the grass *Lolium rigidum*. *Chromosome Res.* **2001**, *9*, 585–590. [[CrossRef](#)] [[PubMed](#)]
55. Lan, H.; Chen, C.-L.; Miao, Y.; Yu, C.-X.; Guo, W.-W.; Xu, Q.; Deng, X.-X. Fragile Sites of ‘Valencia’ Sweet Orange (*Citrus sinensis*) Chromosomes Are Related with Active 45s rDNA. *PLoS ONE* **2016**, *11*, e0151512. [[CrossRef](#)] [[PubMed](#)]
56. Rocha, L.C.; Ferreira, M.T.M.; Cunha, I.M.F.; Mittelman, A.; Techio, V.H. 45S rDNA sites in meiosis of *Lolium multiflorum* Lam.: Variability, non-homologous associations and lack of fragility. *Protoplasma* **2019**, *256*, 227–235. [[CrossRef](#)]
57. Novák, P.; Guignard, M.S.; Neumann, P.; Kelly, L.J.; Mlinarec, J.; Koblížková, A.; Dodsworth, S.; Kovařík, A.; Pellicer, J.; Wang, W.; et al. Repeat-sequence turnover shifts fundamentally in species with large genomes. *Nat. Plants* **2020**, *6*, 1325–1329. [[CrossRef](#)]
58. Lan, T.; Albert, V.A. Dynamic distribution patterns of ribosomal DNA and chromosomal evolution in *Paphiopedilum*, a lady’s slipper orchid. *BMC Plant Biol.* **2011**, *11*, 126. [[CrossRef](#)]
59. Siroký, J.; Lysák, M.A.; Dolezel, J.; Kejnovský, E.; Vyskot, B. Heterogeneity of rDNA distribution and genome size in *Silene* spp. *Chromosome Res.* **2001**, *9*, 387–393. [[CrossRef](#)]
60. Silva, J.C.; Soares, F.A.F.; Sattler, M.C.; Clarindo, W.R. Repetitive sequences and structural chromosome alterations promote intraspecific variations in *Zea mays* L. karyotype. *Sci. Rep.* **2020**, *10*, 8866. [[CrossRef](#)]
61. Zozomová-Lihová, J.; Mandáková, T.; Kovaříková, A.; Mühlhausen, A.; Mummenhoff, K.; Lysak, M.A.; Kovařík, A. When fathers are instant losers: Homogenization of rDNA loci in recently formed *Cardamine* × *schulzii* trigeneric allopolyploid. *New Phytol.* **2014**, *203*, 1096–1108. [[CrossRef](#)]
62. Chiarini, F.E.; Santiñaque, F.F.; Urdampilleta, J.D.; Las Peñas, M.L. Genome size and karyotype diversity in *Solanum* sect. *Acanthophora* (Solanaceae). *Plant Syst. Evol.* **2014**, *300*, 113–125. [[CrossRef](#)]
63. Hasterok, R.; Wolny, E.; Hosiawa, M.; Kowalczyk, M.; Kulak-Książczyk, S.; Książczyk, T.; Heneen, W.K.; Maluszynska, J. Comparative analysis of rDNA distribution in chromosomes of various species of Brassicaceae. *Ann. Bot.* **2006**, *97*, 205–216. [[CrossRef](#)] [[PubMed](#)]
64. Bernardes, E.C.S.; Benko-Iseppon, A.M.; Vasconcelos, S.; Carvalho, R.; Brasileiro-Vidal, A.C. Intra- and interspecific chromosome polymorphisms in cultivated *Cichorium* L. species (Asteraceae). *Genet. Mol. Biol.* **2013**, *36*, 357–363. [[CrossRef](#)] [[PubMed](#)]
65. Huang, J.; Ma, L.; Yang, F.; Fei, S.-z.; Li, L. 45S rDNA regions are chromosome fragile sites expressed as gaps in vitro on metaphase chromosomes of root-tip meristematic cells in *Lolium* spp. *PLoS ONE* **2008**, *3*, e2167. [[CrossRef](#)] [[PubMed](#)]
66. Huang, K.; Rieseberg, L.H. Frequency, origins, and evolutionary role of chromosomal inversions in plants. *Front. Plant Sci.* **2020**, *11*, 296. [[CrossRef](#)]
67. Zhang, S.-J.; Liu, L.; Yang, R.; Wang, X. Genome size evolution mediated by *Gypsy* retrotransposons in Brassicaceae. *Genom. Proteom. Bioinform.* **2020**, *18*, 321–332. [[CrossRef](#)]
68. Liu, Z.; Liu, Y.; Liu, F.; Zhang, S.; Wang, X.; Lu, Q.; Wang, K.; Zhang, B.; Peng, R. Genome-wide survey and comparative analysis of long terminal repeat (LTR) retrotransposon families in four *Gossypium* species. *Sci. Rep.* **2018**, *8*, 9399. [[CrossRef](#)]
69. Raskina, O.; Belyayev, A.; Nevo, E. Activity of the En/Spm-like transposons in meiosis as a base for chromosome repatterning in a small, isolated, peripheral population of *Aegilops speltoides* Tausch. *Chromosome Res.* **2004**, *12*, 153–161. [[CrossRef](#)]
70. Symonová, R.; Majtánová, Z.; Sember, A.; Staaks, G.B.; Bohlen, J.; Freyhof, J.; Rábová, M.; Ráb, P. Genome differentiation in a species pair of coregonine fishes: An extremely rapid speciation driven by stress-activated retrotransposons mediating extensive ribosomal DNA multiplications. *BMC Evol. Biol.* **2013**, *13*, 42. [[CrossRef](#)]
71. Xiong, Z.; Gaeta, R.T.; Edger, P.P.; Cao, Y.; Zhao, K.; Zhang, S.; Pires, J.C. Chromosome inheritance and meiotic stability in allopolyploid *Brassica napus*. *G3 Genes Genomes Genet.* **2020**, *11*, jkaa011. [[CrossRef](#)]

72. Emadzade, K.; Jang, T.-S.; Macas, J.; Kovařík, A.; Novák, P.; Parker, J.; Weiss-Schneeweiss, H. Differential amplification of satellite PaB6 in chromosomally hypervariable *Prospero autumnale* complex (Hyacinthaceae). *Ann. Bot.* **2014**, *114*, 1597–1608. [[CrossRef](#)]
73. Venora, G.; Blangiforti, S.; Frediani, M.; Maggini, F.; Gelati, M.T.; Castiglione, M.R.; Cremonini, R. Nuclear DNA contents, rDNAs, chromatin organization, and karyotype evolution in *Vicia* sect. *faba*. *Protoplasma* **2000**, *213*, 118–125. [[CrossRef](#)]
74. Kolano, B.; McCann, J.; Orzechowska, M.; Siwinska, D.; Temsch, E.; Weiss-Schneeweiss, H. Molecular and cytogenetic evidence for an allotetraploid origin of *Chenopodium quinoa* and *C. berlandieri* (Amaranthaceae). *Mol. Phylogenet. Evol.* **2016**, *100*, 109–123. [[CrossRef](#)] [[PubMed](#)]
75. Löytynoja, A.; Goldman, N. WebPRANK: A phylogeny-aware multiple sequence aligner with interactive alignment browser. *BMC Bioinform.* **2010**, *11*, 579. [[CrossRef](#)] [[PubMed](#)]
76. Collingridge, P.W.; Kelly, S. MergeAlign: Improving multiple sequence alignment performance by dynamic reconstruction of consensus multiple sequence alignments. *BMC Bioinform.* **2012**, *13*, 117. [[CrossRef](#)]
77. Minh, B.Q.; Schmidt, H.A.; Chernomor, O.; Schrempf, D.; Woodhams, M.D.; von Haeseler, A.; Lanfear, R. IQ-TREE 2: New models and efficient methods for phylogenetic inference in the genomic era. *Mol. Biol. Evol.* **2020**, *37*, 1530–1534. [[CrossRef](#)]
78. Maddison, W.P.; Maddison, D.R. Mesquite: A Modular System for Evolutionary Analysis. Version 3.7. Available online: <http://mesquiteproject.org> (accessed on 1 March 2021).
79. Glick, L.; Mayrose, I. ChromEvol: Assessing the pattern of chromosome number evolution and the inference of polyploidy along a phylogeny. *Mol. Biol. Evol.* **2014**, *31*, 1914–1922. [[CrossRef](#)]
80. Dydak, M.; Kolano, B.; Nowak, T.; Siwinska, D.; Maluszynska, J. Cytogenetic studies of three European species of *Centaurea* L. (Asteraceae). *Hereditas* **2009**, *146*, 152–161. [[CrossRef](#)]
81. Unfried, I.; Gruendler, P. Nucleotide sequence of the 5.8S and 25S rRNA genes and of the internal transcribed spacers from *Arabidopsis thaliana*. *Nucleic Acids Res.* **1990**, *18*, 4011. [[CrossRef](#)]
82. Gerlach, W.L.; Dyer, T.A. Sequence organization of the repeating units in the nucleus of wheat which contain 5S rRNA genes. *Nucleic Acids Res.* **1980**, *8*, 4851–4865. [[CrossRef](#)]
83. Kolano, B.; Saracka, K.; Broda-Cnota, A.; Maluszynska, J. Localization of ribosomal DNA and CMA3/DAPI heterochromatin in cultivated and wild *Amaranthus* species. *Sci. Hortic.* **2013**, *164*, 249–255. [[CrossRef](#)]